

Lower Bound on the Capacity of the Continuous-Space SSFM Model of Optical Fiber

Milad Sefidgaran and Mansoor Yousefi

Abstract—The capacity of a discrete-time model of optical fiber described by the split-step Fourier method (SSFM) as a function of the average input power \mathcal{P} and the number of segments in distance K is considered. It is shown that if $K \geq \mathcal{P}^{2/3}$ and $\mathcal{P} \rightarrow \infty$, the capacity of the resulting continuous-space lossless model is lower bounded by $\frac{1}{2} \log_2(1 + \text{SNR}) - \frac{1}{2} + o(1)$, where $o(1)$ tends to zero with the signal-to-noise ratio SNR. As $K \rightarrow \infty$, the intra-channel signal-noise interactions average out to zero due to the law of large numbers and the SSFM model tends to a diagonal phase noise model. It follows that, in contrast to the discrete-space model where there is only one signal degree-of-freedom (DoF) at high powers, the number of DoFs in the continuous-space model is at least half of the input dimension n . Intensity-modulation and direct detection achieves this rate. The pre-log in the lower bound when $K = \mathcal{P}^{1/8}$ is generally characterized in terms of δ .

We consider the SSFM model where the dispersion matrix does not depend on K , e.g., when the step size in distance is fixed. It is shown that the capacity of this model when $K \geq \mathcal{P}^3$ and $\mathcal{P} \rightarrow \infty$ is $\frac{1}{2n} \log_2(1 + \text{SNR}) + o(1)$. Thus, there is only one DoF in this model.

Finally, it is shown that if the nonlinearity parameter $\gamma \rightarrow \infty$, the capacity of the continuous-space model is $\frac{1}{2} \log_2(1 + \text{SNR}) + o(1)$ for any SNR.

Index Terms—Optical fiber, channel capacity, split-step Fourier method.

I. INTRODUCTION

Optical fiber is the medium of choice for high-speed data transmission. Although the general expression for the capacity of the point-to-point channels is derived by Shannon [1], evaluating this expression for the optical fiber channel remains difficult.

There are two effects in optical fiber that impact the capacity in point-to-point channels. First, nonlinearity transforms additive noise to *phase noise* during the propagation. As the amplitude of the input signal tends to infinity, the phase of the output signal tends to a uniform random variable in the zero-dispersion channel [2, Sec. IV]. Second, dispersion converts phase noise to amplitude noise introducing a *multiplicative noise*. The successive application of the phase and multiplicative noise makes signal noise interaction intractable.

The achievable rates of the wavelength-division multiplexing (WDM) vanish at high powers due to treating interference (arising from the application of the linear multiplexing to the nonlinear channel) as noise [3]–[6]. On the other hand, it is shown that the capacity of the discrete-time model of the optical fiber is upper bounded by $\log_2(1 + \text{SNR})$, where SNR is the signal-to-noise ratio [7], [8].

M. Sefidgaran and M. Yousefi are with the Communications and Electronics Department of Télécom Paris (Institut Polytechnique de Paris), Paris, France. E-mails: {milad.sefidgaran,yousefi}@telecom-paris.fr.

The problem of finding the capacity has been investigated for the non-dispersive case in [2], [9]–[11]. It is shown that the asymptotic capacity of this channel is $\frac{1}{2} \log_2(\mathcal{P}) + o(1)$ [2], where \mathcal{P} is the average input signal power.

The capacity of the discrete-time discrete-space SSFM model of the optical fiber with fixed step size as a function of \mathcal{P} is studied in [12]. It is shown that this model tends to a linear fading channel as $\mathcal{P} \rightarrow \infty$, described by a random matrix M . The asymptotic capacity of this model in the lossless case is $\frac{1}{2n} \log_2(\mathcal{P}) + c$ where n is the dimension of the input vector and c is a bounded quantity. As a result, there is only one signal degrees-of-freedom (DoF) at high powers (signal energy) due to signal-noise interaction. However, the model in [12] may not describe realistic fiber where the distance is continuous.

The capacity of the discrete-time discrete-space SSFM model as a function of \mathcal{P} and the number of segments in distance K is studied in [13]. It seems that the analysis in [13] suggests that if K tends to infinity sufficiently fast as $K = \mathcal{P}^{1/4}$ and $\mathcal{P} \rightarrow \infty$, the capacity is lower bounded by $\frac{1}{8} \log_2(\mathcal{P}) + c$ where $c < \infty$.

In this paper, we consider the SSFM model of optical fiber as a function of K and \mathcal{P} . The contributions of the paper are as follows.

a) First, we show that when $K \geq \mathcal{P}^{2/3}$ and $\mathcal{P} \rightarrow \infty$, the off-diagonal terms in the random matrix M_K in [12] tend to zero due to the law of large numbers, and M_K tends to a diagonal matrix with phase noise. As a consequence, the capacity of the resulting lossless continuous-space SSFM model is lower bounded as

$$C(\text{SNR}) \geq \frac{1}{2} \log_2(1 + \text{SNR}) - \frac{1}{2} + o(1), \quad (1)$$

where the term $o(1)$ tends to zero with $\text{SNR} \rightarrow \infty$. This suggests that, unlike the discrete-space SSFM model where asymptotically there is only one DoF and the capacity is essentially finite (for large n), in the continuous-space model the number of DoFs is at least half of the input dimension. In particular, the capacity grows with the input power with pre-log of at least $1/2$. The pre-log in the lower bound when $K = \mathcal{P}^{1/8}$ is generally characterized in terms of δ .

b) Second, we consider the lossless SSFM model in which the dispersion matrix does not depend on K , e.g., when the step size in distance is fixed. It is shown that when $K = \mathcal{P}^{1/8}$, $\delta > 3$, and $\mathcal{P} \rightarrow \infty$, $C(\text{SNR}) = \frac{1}{2n} \log_2(1 + \text{SNR}) + o(1)$. In this case, there is one DoF asymptotically as in [12]. This result shows that in this model, the constant c in [2, Thm. 1] tends to $-\frac{1}{2n} \log_2(\sigma^2 \mathcal{L})$, where $\sigma^2 \mathcal{L}$ is the total noise power.

c) Finally, we consider the SSFM model when the nonlinearity parameter $\gamma = \infty$. It is shown that this channel is a fading channel for any K and \mathcal{P} . As a result, when $K \rightarrow \infty$, $\mathcal{C}(\text{SNR}) = \frac{1}{2} \log_2(1 + \text{SNR}) - \frac{1}{2} + o(1)$ for all SNR in the lossless case.

The paper is organized as follows. The notation is introduced in Section II. The discrete- and continuous-space SSFM models are presented in Section III. The main capacity lower bound is presented in Section IV, which is proved and extended in Sections V and VI. The results are verified by simulation experiments in Section VII and the paper is concluded in Section VIII. Appendix A. provides background on a few mathematical concepts.

II. NOTATION

Real and complex numbers are denoted by \mathbb{R} and \mathbb{C} , respectively, with the imaginary unit $j = \sqrt{-1}$. The real and imaginary part of a complex number x are denoted by $\Re(x)$ and $\Im(x)$, respectively. The magnitude and phase of x are denoted by $|x|$ and $\angle x$. The complex conjugate of $z \in \mathbb{C}$ is z^* . Important scalars are shown with the calligraphic font, e.g., \mathcal{P} for power, \mathcal{C} for the capacity, and \mathcal{L} for the length of the optical fiber.

Bold letters are used to denote vectors, e.g., \mathbf{x} . The p -norm of a vector $\mathbf{x} \in \mathbb{C}^n$ is

$$\|\mathbf{x}\|_p = (|x_1|^p + |x_2|^p + \cdots + |x_n|^p)^{1/p}.$$

The Euclidean norm with $p = 2$ is $\|\mathbf{x}\| \triangleq \|\mathbf{x}\|_2$.

The entries of a sequence of vectors $\mathbf{x}_i \in \mathbb{C}^n$, $i = 1, 2, \dots$, are indexed with convention

$$\mathbf{x}_i = (x_{i,1}, x_{i,2}, \dots, x_{i,n}). \quad (2)$$

The following region in the Euclidean space is used in the paper [12]

$$\mathcal{R}_{\mathcal{T}}^+ = \{\mathbf{x} \in \mathbb{C}^n : |x_l| \geq \mathcal{T}, l = 1, 2, \dots, n\}. \quad (3)$$

The n -sphere is denoted by \mathcal{S}^n . A vector \mathbf{x} in the spherical coordinate is represented by its norm $\|\mathbf{x}\|$ and its direction $\hat{\mathbf{x}} = \mathbf{x}/\|\mathbf{x}\|$. The spherical coordinate system is introduced in Appendix A.

Random variables and their realizations are represented by the upper- and lower-case letters respectively. The probability density function (PDF) of a random variable X is denoted by $P_X(x)$. The expected value of a random variable X is denoted by $\mathbb{E}[X]$. The uniform distribution on the interval $[a, b]$ is denoted by $\mathcal{U}(a, b)$. The PDF of a zero-mean circularly-symmetric complex Gaussian random vector with covariance matrix \mathbf{K} is denoted by $\mathcal{N}_{\mathbb{C}}(0, \mathbf{K})$. The equality of random variables X and Y in distribution is written as $X \stackrel{d}{=} Y$.

A family of PDFs $(P_X(x, \mathcal{P}))_{\mathcal{P} \in \mathbb{R}^+}$, $x \in \mathcal{X}$, with the average cost constraint $\mathbb{E}g(\mathbf{X}) \leq \mathcal{P}$ is said to escape to infinity with $\mathcal{P} \rightarrow \infty$ if [14, Def. 2.4]

$$P(\mathbf{x} \in \mathcal{X} : g(\mathbf{x}) \leq \mathcal{P}_0) = 0,$$

for any $\mathcal{P}_0 > 0$.

A sequence of n numbers x_1, \dots, x_n is shown as $(x_l)_{l=1}^n$ or \mathbf{x}^n . The set of integers $\{1, 2, \dots, n\}$ is denoted by $[n]$. A

sequence of n independent and identically distributed (i.i.d.) random variables drawn from the PDF $P_X(x)$ is presented as $X_l \stackrel{\text{i.i.d.}}{\sim} P_X(x)$.

Deterministic matrices are denoted by upper-case letters with mathrm font, e.g., \mathbf{D} , and random matrices are shown by upper-case letters with mathsf font, e.g., \mathbf{M} . The identity matrix of size n is \mathbf{I}_n .

For a sequence of matrices $(A_i)_{i=1}^m$, the product is defined with convention $\prod_{i=1}^m A_i = A_m A_{m-1} \cdots A_1$. A diagonal matrix \mathbf{R} with diagonal entries R_i is denoted by $\mathbf{R} = \text{diag}(R_1, \dots, R_n)$. The following diagonal matrix is used throughout the paper

$$\mathbf{R}(\theta) \triangleq \text{diag}\left(\left(\exp(j\theta_l)\right)_{l=1}^n\right), \quad (4)$$

where $\theta_l \stackrel{\text{i.i.d.}}{\sim} \mathcal{U}(0, 2\pi)$.

The group of complex-valued $n \times n$ unitary matrices is denoted by \mathbb{U}_n . Some properties of \mathbb{U}_n are reviewed in Appendix A.

Suppose that ν is an equivalence relation on the set $\mathcal{I}_n = \{1, 2, \dots, n\}$, partitioning it into non-empty equivalence classes $\mathcal{I}_1, \mathcal{I}_2, \dots, \mathcal{I}_{m(\nu)}$. The notation $\mathbb{U}_n(\nu)$ is used to denote the group of block diagonal unitary matrices \mathbf{A} in which if the integers r and s does not belong to one partition, then $A_{r,s} = 0$.

Given two functions $f(x) : \mathbb{R} \rightarrow \mathbb{C}$ and $g(x) : \mathbb{R} \rightarrow \mathbb{C}$, we say $f(x) = O(g(x))$ or $g(x) = \Omega(f(x))$, if there exists a finite $c > 0$ and $x_0 > 0$ such that $|f(x)| \leq c|g(x)|$, for all $x \geq x_0$. In addition, $f(x) = o(g(x))$ if for any $c > 0$ there exists a finite $x_0 > 0$ such that $|f(x)| \leq c|g(x)|$, for all $x \geq x_0$.

A sequence of random matrices $(\mathbf{A}_k)_{k=1}^{\infty}$ is said to converge to \mathbf{B} w.r.t norm $\|\cdot\|$ with convergence rate v , if

$$\|\mathbf{A}_k - \mathbf{B}\| \stackrel{d}{=} O(k^{-v}).$$

We say $f(x) : \mathbb{R} \rightarrow \mathbb{R}$ is asymptotically lower bounded by $g(x) : \mathbb{R} \rightarrow \mathbb{R}$, and write $f(x) \geq g(x)$, if

$$\lim_{x \rightarrow \infty} (f(x) - g(x)) \geq 0. \quad (5)$$

III. SPLIT-STEP FOURIER MODEL

In this section, we consider a modified version of the SSFM introduced in [12]. Here, the nonlinearity and noise steps are combined into one step, so that the influence of the additive ASE noise can be seen as phase noise. In what follows, SSFM refers to the modified SSFM.

A. Continuous-time model

Denote the complex envelope of the optical signal at distance z and time t by the $Q(t, z)$. The propagation of the signal in single-mode optical fiber with distributed amplification is governed by the stochastic nonlinear Schrödinger (NLS) equation [12, Eq. 2]

$$\frac{\partial Q}{\partial z} = L_L(Q) + L_N(Q) + N(t, z). \quad (6)$$

Here, L_L is the linear operator

$$L_L(Q) = -j \frac{\beta_2}{2} \frac{\partial^2 Q}{\partial t^2} - \frac{1}{2} \alpha_r * Q(t, z), \quad (7)$$

where β_2 is the second-order chromatic dispersion coefficient, $\alpha_r(t)$ is the residual attenuation coefficient (remained after imperfect amplification), $*$ is convolution resulting from the dependence of the attenuation coefficient with frequency, and $j = \sqrt{-1}$. The operator

$$L_N(Q) = j\gamma|Q|^2Q \quad (8)$$

represents the Kerr nonlinearity, where γ is the nonlinearity parameter. Finally, $N(t, z)$ is zero-mean circularly-symmetric complex Gaussian noise process with covariance matrix

$$\mathbb{E}[N(t, z)N^*(t', z')] = \tilde{\sigma}^2 \delta_{\mathcal{W}}(t - t')\delta(z - z'), \quad (9)$$

where $\delta_{\mathcal{W}}(x) = \mathcal{W} \text{sinc}(\mathcal{W}x)$, $\text{sinc}(x) = \sin(\pi x)/(\pi x)$, \mathcal{W} is the noise bandwidth and $\delta(\cdot)$ is the Dirac delta function. Denote $\sigma \triangleq \tilde{\sigma}\sqrt{\mathcal{W}}$.

The capacity results obtained in this paper are expected to hold for more general linear and nonlinear operators L_L and L_N that take into account other forms of dispersion and nonlinearity. However, we restrict the analysis to (7) and (8).

B. Discrete-time SSFM model

The continuous-time model (6) cannot be discretized by sampling as in the linear channels, because the bandwidth of a signal propagating according to (6) is in general signal-dependent and not finite. However, in practice, the NLS equation can be simulated well using the split-step Fourier method and by over-sampling, yielding a good discrete-time approximation of the continuous-time model.

Discretize a fiber of length \mathcal{L} into K segments of length $\varepsilon = \mathcal{L}/K$ in distance, and $Q(t, \cdot)$ to a vector of length n with step size Δ_t in time. Let $\mathbf{V}_i \in \mathbb{C}^n$ be the input of the spatial segment i , where $\mathbf{V}_1 = \mathbf{X}$ is the channel input and $\mathbf{V}_{K+1} = \mathbf{Y}$ is the channel output.

In segment i of the modified SSFM, the following steps are performed [12].

a) Modified nonlinear step: In this step (6) is solved analytically with $L_L = 0$. Let \mathbf{V}_i and \mathbf{U}_i be the input and output in this step, and $M \rightarrow \infty$ a large integer. The channel $\mathbf{V}_i \mapsto \mathbf{U}_i$ is memoryless with the input output relation [12, Eq. 5]

$$U_{i,l} = (V_{i,l} + W_{i,l}(M)) e^{j\Phi_{i,l}},$$

where $U_{i,l}$ and $V_{i,l}$ are entries of \mathbf{U}_i and \mathbf{V}_i defined based on (2), and $(W_{i,l}(m))_{i,l}$ is a sequence of i.i.d discrete-time Wiener processes with variance $\sigma\sqrt{\mu m}$, $\mu = \varepsilon/M$. The nonlinear phase is

$$\Phi_{i,l} \triangleq \gamma\mu \sum_{r=1}^M \left| V_{i,l} + W_{i,l}(r) \right|^2. \quad (10)$$

Denote $\bar{\mathbf{Z}}_i \triangleq \mathbf{W}_i(M)$.

b) Linear step: In this step (6) is solved analytically with $L_N = 0$ and $N(t, z) = 0$. If \mathbf{U}_i is the input and \mathbf{V}_{i+1} is the

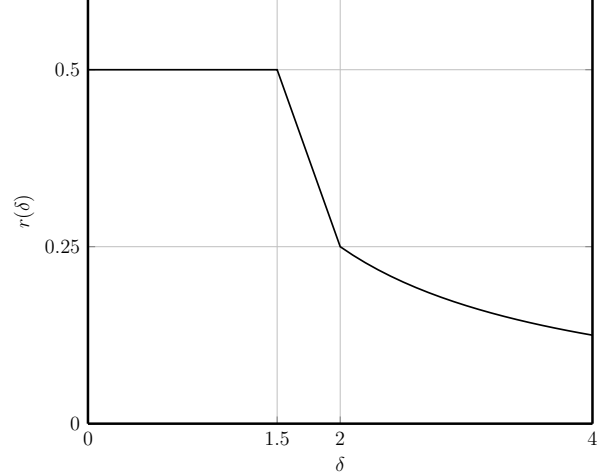


Fig. 1: Pre-log in the capacity lower bound as a function of the growth rate of the number of segments with power.

output of the linear step, the map $\mathbf{U}_i \mapsto \mathbf{V}_{i+1}$ is

$$\mathbf{V}_{i+1} = \mathbf{D}_K \mathbf{U}_i,$$

where \mathbf{D}_K is the (deterministic) dispersion matrix

$$\mathbf{D}_K = \mathbf{F}^{-1} \text{diag} \left((e^{a_l + jb_l})_{l=1}^n \right) \mathbf{F}, \quad (11)$$

where \mathbf{F} is the discrete Fourier transform (DFT) matrix. Further, $a_l = -\mathcal{L}\alpha_l/K$ where $(\alpha_l)_l$ is a discretization of the loss coefficient $\alpha_r(f)$ in frequency f , and

$$b_l = -\frac{\mathcal{L}\beta_2(2\pi)^2}{2K(n\Delta_t)^2} \times \begin{cases} (l-1)^2, & 1 \leq l \leq \frac{n}{2}, \\ (n-l+1)^2, & \frac{n}{2} + 1 \leq l \leq n. \end{cases} \quad (12)$$

Remark 1. The input dimension n is fixed, and should not be confused with the block or codeword length that tends to ∞ .

In what follows, SSFM refers to modified SSFM.

IV. A CAPACITY LOWER BOUND

The capacity of the SSFM model as a function of the average signal power \mathcal{P} and the number of spatial segments K is

$$\mathcal{C}(\mathcal{P}, K) = \max_{p_{\mathbf{X}}(\mathbf{x})} \left\{ \frac{1}{n} I(\mathbf{X}; \mathbf{Y}) : \frac{1}{n} \mathbb{E}[\|\mathbf{X}\|^2] \leq \mathcal{P} \right\}, \quad (13)$$

where $\mathbf{X} \in \mathbb{C}^n$ and $\mathbf{Y} \in \mathbb{C}^n$ are the channel input and output.

The capacity of the continuous-space model is

$$\mathcal{C}(\mathcal{P}) = \lim_{K \rightarrow \infty} \mathcal{C}(\mathcal{P}, K). \quad (14)$$

The main result of this paper is Theorem 1 stating that for sufficiently large number of segments, rate $\frac{1}{2} \log_2(\text{SNR}) - \frac{1}{2}$ is achievable at high SNRs in the continuous-space lossless model.

Theorem 1. The capacity of the SSFM model when $K = \mathcal{P}^{1/\delta}$, $\delta > 0$, and $\mathcal{P} \rightarrow \infty$ is lower bounded as

$$\mathcal{C}(\text{SNR}) \geq r(\delta) \log_2(1 + a \text{SNR}) + O(1), \quad (15)$$

where $\text{SNR} = \mathcal{P}/(\sigma^2 \mathcal{L})$, and the pre-log $r(\delta)$ is

$$r(\delta) = \begin{cases} \frac{1}{2}, & 0 \leq \delta \leq \frac{3}{2}, \\ \frac{3-\delta}{2\delta}, & \frac{3}{2} \leq \delta \leq 2, \\ \frac{1}{2\delta}, & 2 \leq \delta. \end{cases} \quad (16)$$

Here, $a = \zeta e^{2\zeta}/(e^{2\zeta} - 1)$, in which $\zeta = -\bar{\alpha}\mathcal{L}$, where $\bar{\alpha}$ is the average fiber loss in frequency.

In particular, if $K \geq \mathcal{P}^{2/3}$ and $\mathcal{P} \rightarrow \infty$, then

$$\mathcal{C}(\text{SNR}) \geq \frac{1}{2} \log_2 (1 + \text{SNR}) + \frac{1}{2} \log_2 a + o(1), \quad (17)$$

where the term $o(1)$ tends to zero with $\text{SNR} \rightarrow \infty$. For the lossless fiber, $a = 1/2$.

In practice the launch power is finite and K can be chosen to be arbitrarily large. Theorem 1 indicates that rates given by (17) are achievable. In fiber-optic simulations, choosing sufficiently large number of segments in SSFM, the channel capacity is between the lower bound in (17) and $\log_2 (1 + \text{SNR})$ [7], [8].

Theorem 1 indicates that the number of signal DoFs is at least half of the input dimension in the continuous-space model. In contrast, there is only one signal DoF at high powers in the discrete-space SSFM model where $D_K \triangleq D$ is independent of K . The lower bound (1) can be compared with the asymptotic capacity of the discrete-space SSFM model [12, Thm. 1]

$$\mathcal{C}(\mathcal{P}, K) = \begin{cases} \frac{1}{n} \log \log (\mathcal{P}) + O(1), & \text{non-constant loss,} \\ \frac{1}{2n} \log (\mathcal{P}) + O(1), & \text{constant loss,} \end{cases} \quad (18)$$

where there is only one DoF, and the pre-log is $1/2n$ in the lossless model.

The pre-log $1/2\delta$ for $\delta \geq 4$ (corresponding to the third branch in (16)) can be obtained from [13] as well. The maximum pre-log is however $1/2$.

V. PROOF OF THEOREM 1 AND RELATED CAPACITY THEOREMS

In this section, we outline the proof of Theorem 1. In addition, we present a number of capacity theorems for models related to the SSFM. Most of the proofs appear in Section VI.

To study the capacity of the SSFM model, we first study the limit of the channel when the input \mathbf{x} is large, which is a fading channel [12]. We establish the capacity and properties of this fading channel. We next study the capacity of the SSFM model using the results for the fading channel.

A. Capacity of the continuous-space fading model

We begin by considering the limit of the SSFM channel when K is fixed and $\mathcal{P} \rightarrow \infty$. It is shown in [12, Sec. V] that as the input distribution escapes to infinity with power, the SSFM channel with fixed K tends to the following *fading channel*:

$$\mathbf{Y} = \mathbf{M}_K \mathbf{X} + \mathbf{Z}_K, \quad (19)$$

where the random matrix \mathbf{M}_K , representing a multiplicative noise, is independent of \mathbf{X} and given by

$$\mathbf{M}_K = \prod_{i=1}^K (\mathbf{D}_K \mathbf{R}(\boldsymbol{\theta}_i)), \quad (20)$$

where $\boldsymbol{\theta}_i \stackrel{\text{i.i.d.}}{\sim} \mathcal{U}^n(0, 2\pi)$. The expression for the additive noise is

$$\mathbf{Z}_K = \sum_{i=1}^K \left(\prod_{r=i}^K (\mathbf{D}_K \mathbf{R}(\boldsymbol{\theta}_r)) \right) \bar{\mathbf{Z}}_i. \quad (21)$$

where $\bar{\mathbf{Z}}_i \sim \mathcal{N}_{\mathbb{C}}(0, \sigma^2 \epsilon \mathbf{I}_n)$. In the lossless case, (21) is simplified and $\mathbf{Z}_K \sim \mathcal{N}_{\mathbb{C}}(0, \sigma^2 \mathcal{L} \mathbf{I}_n)$.

A special case of the fading channel (19) is the non-coherent memoryless phase noise channel [15]

$$Y_l = e^{j\theta_l} X_l + Z_l, \quad l = 1, 2, \dots, n, \quad (22)$$

where $\theta_l \sim \mathcal{U}(0, 2\pi)$ and $Z_l \sim \mathcal{N}_{\mathbb{C}}(0, \sigma_0^2)$. The capacity of this channel, denoted by \mathcal{C}_P , is [15, Eq. 23]:

$$\mathcal{C}_P(\mathcal{P}) = \frac{1}{2} \log_2 \left(1 + \frac{\mathcal{P}}{2\sigma_0^2} \right) + o(1), \quad (23)$$

where the term $o(1)$ tends to zero with $\mathcal{P} \rightarrow \infty$.

Definition 1. For a dispersion matrix of the form (11), we define the “total dispersion values” $d_l = Kb_l$, $l \in [n]$. Dispersion is finite if $d_l < \infty$ for all l , and infinite if $d_l = \infty$ for all l . Similarly, we define the “total loss values” $\zeta_l = Ka_l$, $l \in [n]$.

Denote the average values of the total loss and dispersion in frequency by

$$\zeta \triangleq \frac{1}{n} \sum_{l=1}^n \zeta_l, \quad d \triangleq \frac{1}{n} \sum_{l=1}^n d_l. \quad (24)$$

Alternatively, $\zeta = -\bar{\alpha}\mathcal{L}$, where $\bar{\alpha} \triangleq (1/n) \sum_{l=1}^n \alpha_l$ is the average fiber loss. If $n \rightarrow \infty$, $\bar{\alpha} = \lim_{F \rightarrow \infty} \frac{1}{F} \int_{-F/2}^{F/2} \alpha_r(f) df$.

For realistic fiber, b_l is given by (12), and dispersion is finite due to factor $1/K$ in (12). In this case, the effect of dispersion locally in a small segment is infinitesimal, and $\lim_{K \rightarrow \infty} \mathbf{D}_K = \mathbf{I}_n$. However, we also consider models where b_l is independent of K ; here the dispersion matrix in each small segment is fixed $\mathbf{D}_K \triangleq D$, and the total dispersion value is infinite as $K \rightarrow \infty$.

Definition 2. Consider a discrete-time channel $\mathbf{X} \mapsto \mathbf{Y}$, where $\mathbf{X}, \mathbf{Y} \in \mathbb{R}^n$, with the average power constraint $\mathbb{E}[\|\mathbf{X}\|^2] \leq n\mathcal{P}$ and capacity $\mathcal{C}(\mathcal{P}, n)$. We say there are $r > 0$ real signal DoFs if the capacity pre-log is r/n , i.e., $\lim_{\mathcal{P} \rightarrow \infty} \mathcal{C}(\mathcal{P}, n)/\log(\mathcal{P}) = r/n$.

Below, we lower bound the capacity of the fading channel (19) with finite or infinite dispersion.

1) *Finite Dispersion*: A core result of this paper is Lemma 1 stating that as $K \rightarrow \infty$, the random matrix \mathbf{M}_K in (19) tends to a diagonal matrix with independent phase noise components.

For a random vector $\boldsymbol{\theta}$, define

$$\mathbf{L}(\boldsymbol{\theta}) \triangleq \mathbf{R}(\boldsymbol{\theta}) \mathbf{C}_1 \mathbf{R}(\boldsymbol{\theta})^{-1}, \quad (25)$$

where $C_1 \triangleq F^{-1} \text{diag}((\zeta_l + jd_l)_{l=1}^n)F$ and $\bar{L} \triangleq \mathbb{E}_{\theta} [L(\theta)]$.

Lemma 1. *The random matrix M_K has the expansion*

$$M_K \stackrel{d}{=} \left(e^{\zeta+jd} I_n + \frac{1}{K} \sum_{i=1}^K L(\theta_i) - \bar{L} \right) R(\theta) + O\left(\frac{1}{K}\right), \quad (26)$$

where θ and θ_i are drawn i.i.d. from $\mathcal{U}^n(0, 2\pi)$. In particular,

$$\lim_{K \rightarrow \infty} M_K \stackrel{d}{=} e^{\zeta} R(\theta). \quad (27)$$

Proof. The proof is given in Section VI-A. \square

Substituting the limit of M_K in (20) into (21), we also obtain $\lim_{K \rightarrow \infty} Z_K = Z$, where $Z \sim \mathcal{N}_{\mathbb{C}}(0, \sigma' I_n)$, $\sigma' = \sigma^2 \mathcal{L}(e^{2\zeta} - 1)/2\zeta$. The following lemma follows.

Lemma 2. *As $K \rightarrow \infty$, the fading channel (19) with finite dispersion tends to n independent phase noise channels*

$$Y_l = e^{\zeta+j\theta_l} X_l + Z_l, \quad l = 1, \dots, n, \quad (28)$$

where $\theta_l \stackrel{i.i.d.}{\sim} \mathcal{U}(0, 2\pi)$ and $Z_l \stackrel{i.i.d.}{\sim} \mathcal{N}_{\mathbb{C}}(0, \eta \sigma^2 \mathcal{L})$, in which

$$\eta = \begin{cases} 1, & \text{for lossless channel,} \\ \frac{e^{2\zeta}-1}{2\zeta}, & \text{otherwise.} \end{cases} \quad (29)$$

The first capacity result in this paper is the following theorem showing that the pre-log of the capacity of the continuous-space fading channel with finite dispersion when $K \rightarrow \infty$ and \mathcal{P} is finite is $1/2$, i.e., there are n real signal DoFs when the input dimension is $2n$.

Theorem 2. *Capacity of the continuous-space fading channel (19) with finite dispersion and SNR satisfies*

$$\lim_{K \rightarrow \infty} \bar{C}(\mathcal{P}, K) = \frac{1}{2} \log_2 (1 + a \text{SNR}) + o(1), \quad (30)$$

where SNR and a are given in Theorem 1.

Proof. The result is obtained by combining Lemmas 1 and 2 and the capacity result (23). \square

Next, we consider the capacity of the finite dispersion fading channel when $K = \sqrt[delta]{\mathcal{P}}$, $\delta > 0$, $\mathcal{P} \rightarrow \infty$. Substituting (26) into (19), (22) is modified to

$$\mathbf{Y} \rightarrow e^{\zeta} R(\theta) \mathbf{X} + \mathbf{Z} + \Delta, \quad \text{as } K \rightarrow \infty,$$

where

$$\begin{aligned} \Delta &= \left\{ \left(\frac{1}{K} \sum_{i=1}^K L(\theta_i) - \bar{L} \right) R(\theta) + O\left(\frac{1}{K}\right) \right\} \mathbf{X} \\ &\stackrel{(a)}{=} O\left(K^{\frac{\delta-1}{2}}\right), \end{aligned}$$

where step (a) is obtained considering $\mathcal{P} = K^\delta$. Here, Δ is generally a full random matrix capturing intra-channel interactions.

If $\delta < 1$, then $\Delta \rightarrow 0$ and $\mathbf{Y} \rightarrow e^{\zeta} R(\theta) \mathbf{X} + \mathbf{Z}$. In this case, the capacity is provided by Theorem 2.

If $\delta > 1$, Δ grows with K and constitutes the dominant stochastic impairment. The following theorem establishes a lower bound on the capacity in this case.

Denote

$$\rho \triangleq \sqrt{\sum_{r=1}^n \left| \sum_{s=1}^n (\zeta_s + jd_s) e^{-\frac{j2\pi rs}{n}} \right|^4}.$$

In the following theorem, we restrict the inputs to the class of random variables for which $h(M_K \mathbf{X})$ is a continuous function of K . A class of such random variables is given in [16, Def. 1,3].

Theorem 3. *Let X_i be i.i.d. random variables, $K = \sqrt[delta]{\mathcal{P}}$, $\delta > 1$, and $\mathcal{P} \rightarrow \infty$. The following results hold for the fading channel (19).*

i. *For any input \mathbf{X}*

$$\begin{aligned} \frac{1}{n} I(\mathbf{X}; \mathbf{Y}) &\geq \frac{1}{2\delta} \log_2(\mathcal{P}) + h(|X_1|) - \mathbb{E} [\log_2 (\|\mathbf{X}\|_4)] \\ &\quad + \frac{1}{2} \log_2 \left(\frac{e^{2\zeta-1}}{2\rho\pi} \right) + o(1), \end{aligned}$$

where $o(1)$ term vanishes with \mathcal{P} .

ii. *In particular if $\mathbf{X} \sim \mathcal{N}_{\mathbb{C}}(0, \mathcal{P} I_n)$ then*

$$\bar{C}(\mathcal{P}, K) \geq \frac{1}{2\delta} \log_2(\mathcal{P}) + \frac{1}{2} \log_2 \left(\frac{e^{2\zeta+1}}{\rho\pi\sqrt{8n}} \right) + o(1).$$

Proof. See Section VI-B. \square

2) *Infinite Dispersion:* We consider the SSFM model when $D_K \triangleq D$ is independent of K . Lemma 3 below shows that, in the lossless infinite dispersion case, as $K \rightarrow \infty$ the random matrix M_K in (19) tends to a random unitary matrix.

Lemma 3. *Let ν be an equivalence relation on the set $\{1, 2, \dots, n\}$, and $\mathbb{U}_n(\nu)$ the smallest subgroup of block diagonal matrices in \mathbb{U}_n that contains D . Then, the distribution of M_K tends to the Haar measure on $\mathbb{U}_n(\nu)$ as $K \rightarrow \infty$.*

Proof. See Section VI-C. \square

In the following assume that D is not a block diagonal matrix (of more than one block), i.e. $\mathbb{U}_n(\nu) = \mathbb{U}_n$.

Decompose the mutual information for the fading channel (19) as:

$$I(\mathbf{X}; \mathbf{Y}) = I(\mathbf{X}; \|\mathbf{Y}\|) + I(\mathbf{X}; \hat{\mathbf{Y}} \|\mathbf{Y}\|). \quad (31)$$

Lemma 3 and Theorem 10 in Appendix A imply that the second term approaches zero as $K \rightarrow \infty$. The conditional PDF of the signal norm is

$$\begin{aligned} P_{\|\mathbf{Y}\| \mid \mathbf{X}} (\|\mathbf{y}\| \mid \mathbf{x}) &= P_{\|\mathbf{Y}\| \mid \|\mathbf{X}\|} (\|\mathbf{y}\| \mid \|\mathbf{x}\|) \\ &= \frac{2\|\mathbf{y}\|^n}{\sigma^2 \mathcal{L} \|\mathbf{x}\|^{n-1}} \exp \left(-\frac{\|\mathbf{y}\|^2 + \|\mathbf{x}\|^2}{\sigma^2 \mathcal{L}} \right) \\ &\quad \times I_{n-1} \left(\frac{2\|\mathbf{x}\| \|\mathbf{y}\|}{\sigma^2 \mathcal{L}} \right), \end{aligned} \quad (32)$$

where $I_m(\cdot)$ is the modified Bessel function of the first kind with order m . Equations (31) and (32) yield the following theorem.

Theorem 4. Suppose that $D \stackrel{\Delta}{=} D_K$ is independent of K and is not a block diagonal matrix. The continuous-space fading channel (19) has one signal DoF with capacity

$$\lim_{K \rightarrow \infty} \bar{C}(\mathcal{P}, K) = \max_{P_{\|\mathbf{x}\|}(\|\mathbf{x}\|)} \left\{ \frac{1}{n} I(\|\mathbf{X}\|; \|\mathbf{Y}\|) : \frac{1}{n} \mathbb{E} [\|\mathbf{X}\|^2] \leq \mathcal{P} \right\},$$

where $P(\|\mathbf{y}\| \|\mathbf{x}\|)$ is given by (32). Moreover, as $\|\mathbf{x}\| \rightarrow \infty$ (32) tends to a Gaussian distribution and

$$\lim_{K \rightarrow \infty} \bar{C}(\mathcal{P}, K) = \frac{1}{2n} \log_2 \left(1 + \frac{\mathcal{P}}{\sigma^2 \mathcal{L}} \right) + o(1),$$

where $o(1)$ term tends to zero with $\mathcal{P} \rightarrow \infty$.

Proof. The result follows from Lemma 3 and its consequences stated above. \square

Remark 2. In general, if $\mathbb{U}_n(\nu)$ is the smallest subgroup of block diagonal matrices containing D , then the capacity of the continuous-space fading channel with infinite dispersion has $m(\nu)$ real signal DoFs.

B. Capacity of the continuous-space SSFM model

In this section, the capacity of the continuous-space SSFM model is investigated in the high power regime, as well as with infinite nonlinearity, and infinite dispersion.

1) *High power regime:* Let $K = \sqrt[\delta]{\mathcal{P}}$, $\delta > 0$, and assume that the input \mathbf{X} escapes to infinity. We show that the limit of the discrete-space SSFM channel where $K \rightarrow \infty$ is a diagonal model with phase noise. The convergence rate to this diagonal model depends on δ . We derive a lower bound on the convergence rate, from which a lower bound on the capacity is established. Denote

$$\mathbf{S}_K \triangleq \text{diag} \left(\left(\exp \left(j \sum_{i=1}^K \Phi_{i,l} \right) \right)_{l=1}^n \right).$$

Lemma 4. Suppose that $K = \sqrt[\delta]{\mathcal{P}}$, $\delta > 0$, and \mathbf{X} escapes to infinity with \mathcal{P} . As $\mathcal{P} \rightarrow \infty$, the SSFM channel tends to

$$\mathbf{Y} = \mathbf{M}_K \mathbf{X} + \mathbf{Z},$$

where $\mathbf{Z} \sim \mathcal{N}_{\mathbb{C}}(0, \eta \sigma^2 \mathcal{L} \mathbf{I}_n)$, η is defined in Lemma 2, and

$$\mathbf{M}_K = e^{\zeta + jd} \mathbf{S}_K + O(K^{-v(\delta)}).$$

Here,

$$v(\delta) + \epsilon' \geq \begin{cases} 5\delta/6, & 0 \leq \delta \leq 1, \\ 1 - \delta/6 - g, & 1 \leq \delta \leq 1.5, \\ 1.5 - \delta/2 - g, & 1.5 \leq \delta \leq 2 \\ & \text{and i.i.d. input,} \\ 0.5, & 2 \leq \delta \leq 3 \\ & \text{and i.i.d. input,} \\ 0.5, & 3 \leq \delta, \end{cases} \quad (33)$$

where $\epsilon' > 0$ can be arbitrarily small and g is a bounded function of δ , K , and \mathbf{X} . \square

Proof. See Section VI-D. \square

Theorem 1 will be proved using Lemma 4 in Section VI-E. The term $O(1)$ in Theorem 1 for $\delta \geq 2$ is given in Theorem 3.

Remark 3. For $0 \leq \delta \leq 1.5$, the dominant term in $O(K^{-v(\delta)})$ is the signal-noise interactions, and for $1.5 \leq \delta \leq 3$, is the intra-channel interactions (between different indices). For $3 < \delta$ both effects are significant.

2) *Infinite nonlinearity:* It is commonly believed that nonlinearity is a distortion that reduces the capacity. In this section we show that when $\gamma = \infty$, the channel has at least n real signal DoFs.

Theorem 5. The capacity of continuous-space SSFM for any \mathcal{P} satisfies

$$\lim_{K \rightarrow \infty} \lim_{\gamma \rightarrow \infty} \mathcal{C}(\mathcal{P}, K) = \frac{1}{2} \log_2 (1 + a \text{SNR}) + o(1), \quad (34)$$

where a is given in Theorem 1 and $o(1)$ term tends to zero with $\mathcal{P} \rightarrow \infty$.

Proof. It is easy to verify that as $\gamma/K \rightarrow \infty$, for any $i \in [K]$ and $l \in [n]$, $\Phi_{i,l} \rightarrow \infty$, and consequently, $\text{mod}(\Phi_{i,l}, 2\pi) \rightarrow \mathcal{U}(0, 2\pi)$, independent of $\Phi_{i',l'}$ in other segment l' or coordinate i' . Hence, the SSFM channel is a finite dispersion fading channel, and Theorem 2 yields the result. \square

3) *Infinite dispersion:* The asymptotic capacity of the discrete-space SSFM channel where $D_K \stackrel{\Delta}{=} D$ is independent of $K < \infty$ is given in (18). In this section, we show that this result holds under the same assumption $D_K \stackrel{\Delta}{=} D$ for the continuous-space lossless SSFM channel as well. Note that with fixed step size, as $K \rightarrow \infty$ the dispersion is infinite.

Theorem 6. Consider the SSFM model when $D_K \stackrel{\Delta}{=} D$ is independent of K . If $K = \sqrt[\delta]{\mathcal{P}}$, $\delta > 3$, and $\mathcal{P} \rightarrow \infty$, then

$$\mathcal{C}(\mathcal{P}) = \frac{1}{2n} \log_2 (1 + \text{SNR}) + o(1),$$

where $o(1)$ term tends to zero with \mathcal{P} .

Proof. Similar to the analysis in [12], it can be shown that if $\mathbb{E} [\|\mathbf{X}\|^2] = n\mathcal{P}$, $\mathcal{P} = K^\delta$, $\delta > 3$, then with high probability $\mathbb{E} [V_{i,l}] = O(K^\delta)$ for all $i \in [K]$ and $l \in [n]$. Furthermore, in the proof of Lemma 4 it is shown that in this case $\text{mod}(\Phi_{i,l}, 2\pi) \rightarrow \mathcal{U}(0, 2\pi)$. Hence, infinite dispersion SSFM channel converges to the infinite dispersion fading channel. The result then follows from Theorem 4. \square

VI. PROOFS

A. Proof of Lemma 1

For matrices A and B define the commutator $[A, B] = ABA^{-1}B^{-1}$. It can be verified with algebraic manipulations that \mathbf{M}_K can be written as

$$\begin{aligned} \mathbf{M}_K &= \prod_{i=1}^K D_K \mathbf{R}(\boldsymbol{\theta}_i) \\ &= \left\{ \prod_{i=2}^K D_K \left[\prod_{l=i}^K \mathbf{R}(\boldsymbol{\theta}_l), D_K \right] \right\} D_K \prod_{l=1}^K \mathbf{R}(\boldsymbol{\theta}_l) \\ &= \left\{ \prod_{i=2}^K D_K \left[\mathbf{R} \left(\sum_{l=i}^K \boldsymbol{\theta}_l \right), D_K \right] \right\} D_K \mathbf{R} \left(\sum_{l=1}^K \boldsymbol{\theta}_l \right). \end{aligned}$$

Since the joint distribution of $\left(\sum_{l=1}^K \theta_l\right)_i$ and θ_i are the same

$$\mathbf{M}_K \stackrel{d}{=} \left\{ \prod_{i=2}^K (\mathbf{D}_K [\mathbf{R}(\theta_i), \mathbf{D}_K]) \right\} \mathbf{D}_K \mathbf{R}(\theta_1). \quad (35)$$

Let

$$\mathbf{C}_m \triangleq \frac{1}{m!} \mathbf{F}^{-1} \operatorname{diag} \left(\left((\zeta_l + jd_l)^m \right)_{l=1}^n \right) \mathbf{F}, \quad (36)$$

and $\bar{\mathbf{C}}_m \triangleq (-1)^m \mathbf{C}_m$. Expand \mathbf{D}_K and \mathbf{D}_K^{-1} in K using the Taylor's theorem

$$\mathbf{D}_K = \mathbf{I}_n + \frac{1}{K} \mathbf{C}_1 + \frac{1}{K^2} \mathbf{C}_2 + O\left(\frac{1}{K^3}\right), \quad (37)$$

$$\mathbf{D}_K^{-1} = \mathbf{I}_n + \frac{1}{K} \bar{\mathbf{C}}_1 + \frac{1}{K^2} \bar{\mathbf{C}}_2 + O\left(\frac{1}{K^3}\right).$$

A simple calculation shows that

$$[\mathbf{R}(\theta_i), \mathbf{D}_K] = \mathbf{I}_n + \frac{\mathbf{L}(\theta_i) + \bar{\mathbf{C}}_1}{K} + O\left(\frac{1}{K^2}\right).$$

Using (37) and $\mathbf{C}_1 + \bar{\mathbf{C}}_1 = 0$,

$$\mathbf{D}_K [\mathbf{R}(\theta_i), \mathbf{D}_K] = \mathbf{I}_n + \frac{\mathbf{L}(\theta_i)}{K} + O\left(\frac{1}{K^2}\right).$$

Combining (35) and the above relation results in

$$\begin{aligned} \mathbf{M}_K &= \left\{ \prod_{i=2}^K \left(\mathbf{I}_n + \frac{\mathbf{L}(\theta_i)}{K} + O\left(\frac{1}{K^2}\right) \right) \right\} \mathbf{D}_K \mathbf{R}(\theta_1) \\ &= \left\{ \prod_{i=2}^K \left(\mathbf{I}_n + \frac{\bar{\mathbf{L}}}{K} + \frac{\mathbf{L}(\theta_i) - \bar{\mathbf{L}}}{K} \right) \right\} \mathbf{R}(\theta_1) + O\left(\frac{1}{K}\right) \\ &= \left(\left\{ \prod_{i=2}^K \left(\mathbf{I}_n + \frac{\bar{\mathbf{L}}}{K} \right) \right\} + \frac{\sum_{i=2}^K (\mathbf{L}(\theta_i) - \bar{\mathbf{L}})}{K} \right) \mathbf{R}(\theta_1) \\ &\quad + O\left(\frac{1}{K}\right) \\ &\stackrel{(a)}{=} \left(e^{\bar{\mathbf{L}}} + \frac{1}{K} \sum_{i=1}^K \mathbf{L}(\theta_i) - \bar{\mathbf{L}} \right) \mathbf{R}(\theta_1) + O\left(\frac{1}{K}\right). \end{aligned}$$

where (a) is obtained using

$$\left(1 + \frac{\bar{\mathbf{L}}}{K} \right)^K = e^{\bar{\mathbf{L}}} + O\left(\frac{1}{K}\right).$$

Finally, since $e^{\bar{\mathbf{L}}} = e^{(\zeta+jd)\mathbf{I}_n} = e^{\zeta+jd}\mathbf{I}_n$,

$$\mathbf{M}_K \stackrel{d}{=} \left(e^{\zeta+jd}\mathbf{I}_n + \frac{1}{K} \sum_{i=1}^K \mathbf{L}(\theta_i) - \bar{\mathbf{L}} \right) \mathbf{R}(\theta) + O\left(\frac{1}{K}\right).$$

B. Proof of Theorem 3

Part i: Define the matrix $\Delta \triangleq \frac{1}{K} \sum_{m=1}^K \mathbf{L}(\theta_m) - \bar{\mathbf{L}}$. Considering (25), Δ_{rr} is deterministic and thus zero. If $r \neq l$,

$$\Delta_{lr} = \frac{(C_1)_{lr}}{K} \sum_{i=1}^K e^{j(\theta_{i,l} - \theta_{i,r})}$$

$$\rightarrow \frac{(C_1)_{lr}}{\sqrt{K}} T_{lr}$$

where $T_{lr} \sim \mathcal{N}_{\mathbb{C}}(0, 1)$ and we used the central limit theorem. This yields

$$\mathbf{M}_K \stackrel{d}{=} e^{\zeta} \mathbf{R}(\theta) + O\left(\frac{1}{\sqrt{K}}\right).$$

Hence,

$$\begin{aligned} h(\mathbf{Y}) &= h(\mathbf{M}_K \mathbf{X}) + o(1) \\ &= n \log_2 (e^{\zeta} \mathbf{R}(\theta) \mathbf{X}) + o(1) \\ &= n \log_2 (2\pi e^{2\zeta}) + nh(|X_1|) + n\mathbb{E}[\log_2(|X_1|)] + o(1), \end{aligned} \quad (38)$$

where $o(1)$ term vanishes with $K \rightarrow \infty$ and $\mathcal{P}/K \rightarrow \infty$.

Next, we bound the conditional entropy part as:

$$h(\mathbf{Y}|\mathbf{X}) \leq \sum_{l=1}^n h(Y_l|\mathbf{X}). \quad (39)$$

The output Y_l can be written as

$$Y_l \stackrel{d}{=} e^{\zeta+j(d+\theta_l)} X_l + \frac{e^{j\theta_l}}{\sqrt{K}} \sum_{r \neq l} (C_1)_{lr} T_{lr} X_r + \sqrt{\eta} Z_l,$$

where $\theta_l \sim \mathcal{U}(0, 2\pi)$ and η is given in (29). Note that for a fixed l , $(T_{l,r})_r$ are independent. Hence, given $\mathbf{X} = \mathbf{x}$,

$$\sum_{r \neq l} (C_1)_{lr} x_r T_{lr} \stackrel{d}{=} \|\mathbf{x}\|_4 T_l,$$

where $T_l \sim \mathcal{N}_{\mathbb{C}}(0, \sigma_{T_l}^2)$, and

$$\begin{aligned} \sigma_{T_l}^2 &= \frac{1}{\|\mathbf{x}\|_4^2} \sum_{r \neq l} |(C_1)_{lr}|^2 |x_r|^2 \\ &\stackrel{(a)}{\leq} \sqrt{\sum_{r \neq l} |(C_1)_{lr}|^4} \\ &\stackrel{(b)}{\leq} \rho. \end{aligned}$$

Step (a) is derived using the Cauchy–Schwarz inequality. Step (b) follows from the structure of C_1 . Thus, conditioned on $\mathbf{X} = \mathbf{x}$,

$$Y_l \stackrel{d}{=} e^{\zeta+j\theta_l} x_l + \frac{e^{j\theta_l} \|\mathbf{x}\|_4}{\sqrt{K}} T_l + \sqrt{\eta} Z_l.$$

Now, the conditional entropy can be bounded as following

$$\begin{aligned} h(Y_l|\mathbf{X}) &\leq h \left(e^{\zeta+j\theta_l} X_l + \frac{e^{j\theta_l} \|\mathbf{x}\|_4}{\sqrt{K}} T_l \mid \mathbf{X} \right) + O\left(\sqrt{\frac{K}{\mathcal{P}}}\right) \\ &= \log_2(\pi) + O\left(\sqrt{\frac{K}{\mathcal{P}}}\right) \\ &\quad + h \left(\left| e^{\zeta} X_l + \frac{\|\mathbf{x}\|_4}{\sqrt{K}} T_l \right|^2 \mid \mathbf{X} \right) \\ &= \log_2(\pi) + O\left(\sqrt{\frac{K}{\mathcal{P}}}\right) \end{aligned}$$

$$\begin{aligned}
& + h\left(\frac{2e^\zeta |X_l| \|\mathbf{X}\|_4}{\sqrt{K}} \Re(T_l e^{-j\angle X_l}) + \frac{\|\mathbf{X}\|_4^2}{K} |T_l|^2 \middle| \mathbf{X}\right) \\
& = \log_2(\pi) + O\left(\sqrt{\frac{K}{\mathcal{P}}}\right) + O\left(\frac{1}{\sqrt{K}}\right) \\
& \quad + h\left(\frac{2e^\zeta |X_l| \|\mathbf{X}\|_4}{\sqrt{K}} \Re(T_l e^{-j\angle X_l}) \middle| \mathbf{X}\right) \\
& = \log_2\left(\frac{2e^\zeta \pi}{\sqrt{K}}\right) + O\left(\sqrt{\frac{K}{\mathcal{P}}}\right) + O\left(\frac{1}{\sqrt{K}}\right) \\
& \quad + \mathbb{E}[\log_2(|X_l| \|\mathbf{X}\|_4)] + h(\Re(T_l) \middle| \mathbf{X}) \\
& \leq \log_2\left(\frac{2e^\zeta \pi}{\sqrt{K}}\right) + O\left(\sqrt{\frac{K}{\mathcal{P}}}\right) + O\left(\frac{1}{\sqrt{K}}\right) \\
& \quad + \mathbb{E}[\log_2(|X_l| \|\mathbf{X}\|_4)] + \frac{1}{2} \log_2(2\pi e\rho).
\end{aligned}$$

This relation together with (38) and (39) yields the first part of the theorem.

Part ii: For $\mathbf{X} \sim \mathcal{N}_{\mathbb{C}}(0, \mathcal{P}\mathbf{I}_n)$,

$$h(\mathbf{R}(\boldsymbol{\theta})\mathbf{X}) = h(\mathbf{X}) = n \log_2(2\pi e \mathcal{P}). \quad (40)$$

Moreover,

$$\begin{aligned}
& \mathbb{E}[\log_2(|X_1|) + \log_2(\|\mathbf{X}\|_4)] \\
& = \frac{1}{2} \log_2(\mathbb{E}[|X_1|^2]) + \frac{1}{4} \log_2(\mathbb{E}[\|\mathbf{X}\|_4^4]) + O\left(\frac{1}{\mathcal{P}}\right) \\
& = \frac{1}{2} \log_2(\mathcal{P}) + \frac{1}{4} \log_2(2n\mathcal{P}^2) + O\left(\frac{1}{\mathcal{P}}\right) \\
& = \log_2(\mathcal{P}) + \frac{1}{4} \log_2(2n) + O\left(\frac{1}{\mathcal{P}}\right).
\end{aligned}$$

This, together with (40) and the first part of theorem implies that

$$\frac{1}{n} I(\mathbf{X}; \mathbf{Y}) \geq \frac{1}{2} \log_2(K) + \frac{1}{2} \log_2\left(\frac{e^{2\zeta+1}}{\rho\pi\sqrt{8n}}\right) + o(1),$$

where $o(1)$ term tends to zero with $K \rightarrow \infty$ and $\mathcal{P}/K \rightarrow \infty$. The proof is complete by setting $K = \sqrt[4]{\mathcal{P}}$.

C. Proof of Lemma 3

The proof is based on Theorem 11 in Appendix A. The reader is referred to Appendix A for the notation used in this section.

Let $\mathbf{T} \triangleq \mathbf{DR}(\boldsymbol{\theta})$. Clearly, \mathbf{T} is a unitary matrix. Denote the probability measure of \mathbf{T} by μ . We show that the following two conditions of Theorem 11 hold.

Condition 1. Denote the smallest closed subgroup of \mathbb{U}_n that contains support of μ , i.e. $\mathcal{S}(\mu)$, as \mathbb{H} . Moreover, denote the smallest subgroup of block diagonal matrices that contains \mathbf{D} as $\mathbb{U}_n(\nu)$.

The first condition to verify is $\mathbb{H} = \mathbb{U}_n(\nu)$. This condition is needed, because if $\mathbb{H} \subset \mathbb{U}_n(\nu)$, then the product of instances of \mathbf{T} will not be in \mathbb{H} . Hence, the probability measure of the product of K i.i.d. instances of \mathbf{T} would not be a Haar measure on $\mathbb{U}_n(\nu)$.

By letting $\boldsymbol{\theta} = (0, \dots, 0)$, we have $\mathbf{D} \in \mathbb{H}$, and thus $\mathbf{D}^{-1} \in \mathbb{H}$, and $\mathbf{D}^{-1}\mathbf{DR}(\boldsymbol{\theta}) = \mathbf{R}(\boldsymbol{\theta}) \in \mathbb{H}$. Hence, \mathbb{H} contains all diagonal unitary matrices including the matrix \mathbf{D} . Since the

smallest block diagonal subgroup that contains \mathbf{D} is $\mathbb{U}_n(\nu)$, Theorem 7 in Appendix A implies $\mathbb{H} = \mathbb{U}_n(\nu)$.

Condition 2. The next condition to verify is that μ is not normally aperiodic. This means that $\mathcal{S}(\mu)$ is not contained in a (left or right) coset of a proper closed normal subgroup of $\mathbb{U}_n(\nu)$. To see why this condition is needed, by contradiction suppose that there exists a proper closed normal subgroup \mathbb{H} of $\mathbb{U}_n(\nu)$ and $\mathbf{V} \in \mathbb{U}_n(\nu)$, such that $\mathcal{S}(\mu) \subseteq \mathbf{V}\mathbb{H}$ or $\mathcal{S}(\mu) \subseteq \mathbb{H}\mathbf{V}$, or equivalently $\mathbf{V}^{-1}\mathcal{S}(\mu) \subseteq \mathbb{H}$ or $\mathcal{S}(\mu)\mathbf{V}^{-1} \subseteq \mathbb{H}$. Suppose that

$$V^{-1} = \mathbf{DR}(\boldsymbol{\theta}_r) \cdots \mathbf{DR}(\boldsymbol{\theta}_1). \quad (41)$$

Consider all matrices $\mathbf{M} = \prod_{i=r+1}^{\infty} \mathbf{DR}(\boldsymbol{\theta}_j) V^{-1}$. The second condition states that the smallest closed normal subgroup that contains these matrices is $\mathbb{U}_n(\nu)$. In other words, starting from any r initial steps, all possible unitary matrices in $\mathbb{U}_n(\nu)$ can be reached.

To verify the second condition, we consider the cases $\mathbf{V}^{-1}\mathcal{S}(\mu) \subseteq \mathbb{H}$ or $\mathcal{S}(\mu)\mathbf{V}^{-1} \subseteq \mathbb{H}$ separately.

Left Coset: In this case, $\mathbf{V}^{-1}\mathbf{D}$ and the subgroup of diagonal matrices belong to \mathbb{H} . Suppose that there exists a $\mathbf{W} \in \mathbb{U}_n(\nu)$ such that $\mathbf{W} \notin \mathbb{H}$ and $\mathbf{W} = \mathbf{Q}\Gamma\mathbf{Q}^{-1}$, where Γ is a diagonal matrix. However, since \mathbb{H} is a normal subgroup of $\mathbb{U}_n(\nu)$ and $\Gamma \in \mathbb{H}$, then $\mathbf{W} = \mathbf{Q}\Gamma\mathbf{Q}^{-1} \in \mathbb{H}$, which is a contradiction.

Right Coset: Since $\mathbf{DR}(\boldsymbol{\theta}_1)V^{-1} \in \mathbb{H}$ and $\mathbf{DR}(\boldsymbol{\theta}_2)V^{-1} \in \mathbb{H}$, we have $\mathbf{DR}(\boldsymbol{\theta}_1 - \boldsymbol{\theta}_2)\mathbf{D}^{-1} \in \mathbb{H}$. Hence, for any $\boldsymbol{\theta}$, $\mathbf{DR}(\boldsymbol{\theta})\mathbf{D}^{-1} \in \mathbb{H}$. Similar to the previous case, by contradiction suppose that there exists $\mathbf{W} \in \mathbb{U}_n(\nu)$ such that $\mathbf{W} \notin \mathbb{H}$ and $\mathbf{W} = \mathbf{Q}\Gamma\mathbf{Q}^{-1}$, where Γ is a diagonal matrix. However, since \mathbb{H} is a normal subgroup of $\mathbb{U}_n(\nu)$, $\mathbf{Q}\mathbf{D}^{-1} \in \mathbb{U}_n(\nu)$, and $\mathbf{D}\mathbf{G}\mathbf{D}^{-1} \in \mathbb{H}$, thus $\mathbf{W} = (\mathbf{Q}\mathbf{D}^{-1})\mathbf{D}\Gamma\mathbf{D}^{-1}(\mathbf{D}\mathbf{Q}^{-1}) \in \mathbb{H}$, which is a contradiction.

D. Proof of Lemma 4

We prove this lemma by induction on the segment index i . Let $\mathbf{X} = K^{\frac{1}{2}}\mathbf{X}'$. For $i \in [K]$, denote

$$\Phi(i) \triangleq \text{diag}\left(\left(j\Phi_{i,l}\right)_{l=1}^n\right),$$

where the nonlinear phase $\Phi_{i,l}$ is given in (10). Define also

$$\mathbf{M}_{i,K} \triangleq \prod_{t=1}^i (\mathbf{D}_K \Phi(t)) = \mathbf{D}_K \Phi(i) \mathbf{M}_{i-1,K},$$

$$\mathbf{Z}_i \triangleq \sum_{t=1}^i \left(\left(\prod_{s=t}^i (\mathbf{D}_K \Phi(s)) \right) \bar{\mathbf{Z}}_t \right) = \mathbf{D}_K \Phi(i) (\mathbf{Z}_{i-1} + \bar{\mathbf{Z}}_i),$$

where $\mathbf{M}_{0,K} \triangleq \mathbf{I}_n$ and $\mathbf{Z}_0 \triangleq 0$. Note that $\mathbf{M}_{K,K} = \mathbf{M}_K$. The output of the i -th segment can be written as

$$\mathbf{V}_{i+1} = \mathbf{M}_{i,K} \mathbf{X} + \mathbf{Z}_i. \quad (42)$$

First, we expand $\mathbf{M}_{i,K}$ similar to the analysis in the proof of Lemma 1. For $t \in [i]$, denote

$$\mathbf{R}_i(t) \triangleq \text{diag}\left(\left(\exp(j \sum_{s=t}^i \Phi_{s,l})\right)_{l=1}^n\right),$$

$$\mathbf{L}_i(t) \triangleq \mathbf{R}_i(t) \mathbf{C}_1 \mathbf{R}_i(t)^{-1},$$

and

$$\Delta_i \triangleq \frac{1}{K} \sum_{t=1}^i \mathbf{L}_i(t) - \frac{i}{K} (\zeta + jd) \mathbf{I}_n,$$

where \mathbf{C}_1 is defined in (36). Expand $\mathbf{M}_{i,K}$ as:

$$\begin{aligned} \mathbf{M}_{i,K} &= \left\{ \prod_{t=2}^i (\mathbf{D}_K [\mathbf{R}_i(t), \mathbf{D}_K]) \right\} \mathbf{D}_K \mathbf{R}_i(1) \\ &= \left\{ \prod_{t=2}^i \left(\mathbf{I}_n + \frac{1}{K} \mathbf{L}_i(t) \right) \right\} \mathbf{R}_i(1) + O(K^{-1}) \\ &= \left(e^{\frac{i}{K}(\zeta+jd)} \mathbf{I}_n + \frac{1}{K} \sum_{t=1}^i \mathbf{L}_i(t) - \frac{i}{K} (\zeta + jd) \mathbf{I}_n \right) \mathbf{R}_i(1) \\ &\quad + O(K^{-1}) \\ &= e^{\frac{i}{K}(\zeta+jd)} \mathbf{R}_i(1) + \Delta_i \mathbf{R}_i(1) + O(K^{-1}). \end{aligned} \quad (43)$$

Note that $\mathbf{R}_K(1) = \mathbf{S}_K$.

We shall prove that for each i :

- *Claim 1.* For $l, l' \in [n]$,

$$(\Delta_i)_{l,l'} = O\left(K^{-v(\delta)}\right), \quad (44)$$

where $v(\delta)$ satisfies (33).

- *Claim 2.* For $l \in [n]$ and $t \in [i]$,

$$\sum_{s=t}^i \Phi_{s,l} - (i-t+1)\gamma\varepsilon|X_l|^2 \rightarrow 0, \quad (45)$$

when

$$i \leq \begin{cases} K^{1-\frac{\delta}{3}-\epsilon'}, & 0 \leq \delta \leq 1.5, \\ K^{2-\delta-\epsilon'}, & 1.5 \leq \delta \leq 2. \end{cases} \quad (46)$$

- *Claim 3.* If i satisfies (46), then $v(\delta)$ in (44) is bounded by

$$v(\delta) \geq \begin{cases} \delta, & 0 \leq \delta \leq 1, \\ 1-g, & 1 \leq \delta \leq 2. \end{cases} \quad (47)$$

Once proven, the claims hold for any i consecutive segments starting from any segment t .

Note that above Claim 1-3 yield

$$\lim_{K \rightarrow \infty} \mathbf{Z}_K \stackrel{(d)}{\equiv} \mathbf{Z},$$

where $\mathbf{Z} \in \mathbb{C}^n$ and $\mathbf{Z} \sim \mathcal{N}_{\mathbb{C}}(0, \eta\sigma^2 \mathcal{L} \mathbf{I}_n)$.

For $i = 1$, Claim 1-3 hold, since

$$\mathbf{M}_{1,K} = \mathbf{D}_K \Phi(1) = e^{\frac{1}{K}(\zeta+jd)} \Phi(1) + O(K^{-1}).$$

Assume that Claim 1-3 hold for $i \in [r-1]$. We need to show that they hold for $i = r$ as well.

Denote

$$\mathbf{E}_t \triangleq e^{-(\zeta+jd)\frac{t-1}{K}} \mathbf{R}_{t-1}^*(1) \bar{\mathbf{Z}}_t = O\left(K^{-1/2}\right). \quad (48)$$

Using the assumption of the induction (44) together with (43) and (42), the nonlinear phase $\Phi_{i+1,l}$, where $i \in [r-1]$, can

be expanded as:

$$\begin{aligned} \Phi_{i+1,l} &= \gamma\varepsilon|V_{i+1,l}|^2 + 2\gamma\varepsilon\sqrt{\varepsilon}\Re(V_{i+1,l}^* Z'_{i+1,l}) + \gamma\varepsilon^2|Z''_{i+1,l}|^2 \\ &= \gamma\varepsilon|V_{i+1,l}|^2 + O\left(K^{\frac{\delta-3}{2}}\right) \\ &\stackrel{(a)}{=} \gamma\varepsilon e^{\frac{2i}{K}\zeta} |X_l|^2 + O\left(K^{\frac{\delta-3}{2}}\right) \\ &\quad + 2\gamma\varepsilon \sum_{l' \neq l} \Re \left[\left(e^{\frac{i}{K}(\zeta+jd)} \mathbf{R}_i(1) \mathbf{X} \right)_l^* (\Delta_{i,K})_{l,l'} X_{l'} \right] \\ &\quad + 2\gamma\varepsilon \Re \left[\left(e^{\frac{i}{K}(\zeta+jd)} \mathbf{R}_i(1) \mathbf{X} \right)_l^* Z_{i,l} \right] \\ &= \gamma\varepsilon e^{\frac{2i}{K}\zeta} |X_l|^2 + O\left(K^{\frac{\delta-3}{2}}\right) \\ &\quad + 2\gamma\varepsilon \sum_{l' \neq l} \Re \left[\left(e^{\frac{i}{K}(\zeta+jd)} \mathbf{R}_i(1) \mathbf{X} \right)_l^* (\Delta_{i,K})_{l,l'} X_{l'} \right] \\ &\quad + 2\gamma\varepsilon e^{\frac{2i}{K}\zeta} \Re \left[X_l^* \sum_{t=1}^i E_{t,l} \right]. \end{aligned} \quad (49)$$

Here step (a) follows by substituting (42) and (43) into the previous line. Variables $Z'_{i+1,l}$ and $Z''_{i+1,l}$ denote Gaussian noises with variances that do not depend on K and $E_{t,l}$ is defined in (48).

The term

$$2\gamma\varepsilon \sum_{l' \neq l} \Re \left[\left(e^{\frac{i}{K}(\zeta+jd)} \mathbf{R}_i(1) \mathbf{X} \right)_l^* (\Delta_{i,K})_{l,l'} X_{l'} \right],$$

captures intra-channel interactions, while the terms

$$2\gamma\varepsilon e^{\frac{2i}{K}\zeta} \Re \left[X_l^* \sum_{t=1}^i E_{t,l} \right],$$

and

$$2\gamma\varepsilon\sqrt{\varepsilon} \Re \left[\left(e^{\frac{i}{K}(\zeta+jd)} \mathbf{R}_i(1) \mathbf{X} \right)_l^* Z'_{i+1,l} \right],$$

represent the signal-noise interactions.

To show Claims 1 and 3, note that $(\Delta_r)_{l,l}$, $l \in [n]$, is equal to zero, with probability one. It remains to show that the off-diagonal elements are $O(K^{-v(\delta)})$. We show this for element (1, 2); the proof is similar for other elements. This element is equal to

$$(\Delta_r)_{1,2} = \frac{(\mathbf{C}_1)_{1,2}}{K} \sum_{i=1}^r e^{j \sum_{s=i}^r (\Phi_{s,1} - \Phi_{s,2})}. \quad (50)$$

The rest of the proof is presented for different ranges of δ , and for $\zeta = 0$, separately. Since in general, for $i \in [K]$,

$$e^{\frac{i}{K}\zeta} \mathbf{X} = K^{\frac{\delta'}{2}} \mathbf{X}', \quad (51)$$

where

$$\delta' = \delta + \frac{2i\zeta}{K \ln(K)} \rightarrow \delta.$$

It can be shown that asymptotically as $K \rightarrow \infty$ the effect of loss in the convergence rate of Δ_r vanishes.

• *Case 0 < $\delta < 1$:* In this case, first for $r \leq K^{1-\delta/3-\epsilon'}$, we prove Claims 2 and 3, and consequently Claim 1 follows. Then using this result, we prove Claim 1 for $r > K^{1-\delta/3-\epsilon'}$ as well.

Assume that $r \leq K^{1-\delta/3-\epsilon'}$. We argue first for $t \in [r]$, Claim 2 holds, from which Claims 1 and 3 are then concluded. Let

$$Q_l \triangleq \gamma \mathcal{L} |X'_l|^2, \quad l \in [n].$$

Using the induction assumption (44) and since $r - t + 1 \leq K^{1-\delta/3-\epsilon'}$,

$$\begin{aligned} & \sum_{s=t}^r \Phi_{s,l} \\ &= (r-t+1)K^{\delta-1}Q_l \\ &+ 2\gamma\varepsilon \Re \left[X_l^* \left(\sum_{s=1}^{t-1} (r-t+1)E_{s,l} + \sum_{s=t}^{r-1} (r-s)E_{s,l} \right) \right] \\ &+ O\left((r-t+1)K^{\delta-1-v(\delta)}\right) + O\left((r-t+1)K^{\frac{\delta-3}{2}}\right) \\ &\stackrel{(a)}{=} (r-t+1)K^{\delta-1}Q_l + O\left(K^{-\delta/3-2\epsilon'}\right) + O\left(K^{\frac{\delta-3}{6}-\epsilon'}\right) \\ &+ O\left(K^{\delta/2-1-1/2}A\right) \\ &= (r-t+1)K^{\delta-1}Q_l + O\left(K^{-\delta/3-2\epsilon'}\right) + O\left(K^{\frac{\delta-3}{6}-\epsilon'}\right) \\ &+ O\left(K^{-3\epsilon'/2}\right) \\ &\rightarrow (r-t+1)K^{\delta-1}Q_l, \end{aligned} \quad (52)$$

where (a) holds due to assumption of induction (47) and

$$\begin{aligned} A &\triangleq \left((t-1)(r-t+1)^2 + \sum_{l=1}^{r-t} l^2 \right)^{1/2} \\ &= O\left(r^{3/2}\right). \end{aligned}$$

This proves Claim 2. Note that as can be seen in the above calculations, due to signal-noise interactions, at most $K^{1-\delta/3-\epsilon'}$ consecutive terms $\sum_{s=t}^r \Phi_{s,l}$ constitute arithmetic series. For small values of noise, it can be seen that the above argument almost holds for any $r \leq K^{1-\epsilon'}$, except for very large values of K , when $K \gg (\gamma \mathcal{L}^{3/2} \sigma)^{-2/\delta}$.

Now, to show Claim 3, by denoting $Q \triangleq Q_1 - Q_2$ and due to (52),

$$\begin{aligned} (\Delta_r)_{1,2} &= \frac{(\mathbf{C}_1)_{1,2}}{K} \sum_{i=1}^r e^{j \sum_{s=i}^r (\Phi_{s,1} - \Phi_{s,2})} \\ &= \frac{(\mathbf{C}_1)_{1,2} e^{j K^{\delta-1} Q} (e^{j K^{2\delta/3-\epsilon'} Q} - 1)}{K (e^{j K^{\delta-1} Q} - 1)}. \end{aligned}$$

Furthermore, since for $0 \leq \delta \leq 1$,

$$e^{j K^{\delta-1} Q} - 1 = O\left(K^{\delta-1}\right),$$

then

$$|(\Delta_r)_{1,2}| \leq |(\mathbf{C}_1)_{1,2}| O\left(K^{-\delta}\right),$$

which completes the proof of Claim 3 and consequently Claim 1.

For $r > K^{1-\delta/3-\epsilon'}$, similarly it can be verified that for each

$K^{1-\delta/3-\epsilon'}$ consecutive terms,

$$\sum_{i=t_1}^{t_2} e^{j \sum_{s=i}^r (\Phi_{s,1} - \Phi_{s,2})} = O\left(K^{1-\delta}\right),$$

where $t_2 = t_1 + K^{1-\delta/3-\epsilon'}$. Hence

$$\begin{aligned} |(\Delta_r)_{1,2}| &\leq |(\mathbf{C}_1)_{1,2}| O\left(K^{\delta/3+\epsilon'} K^{1-\delta} K^{-1}\right) \\ &= |(\mathbf{C}_1)_{1,2}| O\left(K^{-2\delta/3+\epsilon'}\right). \end{aligned}$$

The above bound can be improved using the following approach. When t consecutive terms form a geometric series, then

$$\begin{aligned} & \sum_{i=m-t+1}^m e^{j \sum_{s=i}^r (\Phi_{s,1} - \Phi_{s,2})} \\ &= \frac{e^{j \sum_{s=m-t}^r (\Phi_{s,1} - \Phi_{s,2})} - e^{j \sum_{s=m}^r (\Phi_{s,1} - \Phi_{s,2})}}{e^{j K^{\delta-1} Q} - 1}. \end{aligned}$$

On the other hand, if $t_2 - t_1 \geq K^{1-\delta/3+\epsilon'}$, then similar to the analysis in (52),

$$\begin{aligned} & \sum_{s=t_1}^{t_2-1} \Phi_{s,l} \\ &= (t_2 - t_1)K^{\delta-1}Q_l \\ &+ 2\gamma\varepsilon \Re \left[X_l^* \left(\sum_{s=1}^{t_1-1} (t_2 - t_1)E_{s,l} + \sum_{s=t_1}^{t_2-1} (t_2 - s)E_{s,l} \right) \right] \\ &+ O\left((t_2 - t_1)K^{\delta-1-v(\delta)}\right) + O\left((t_2 - t_1)K^{\frac{\delta-3}{2}}\right). \end{aligned}$$

The second term on the RHS of the above relation is non-deterministic given the input and is of order

$$\Omega\left((t_2 - t_1)^{\frac{3}{2}} K^{\frac{\delta-3}{2}}\right) \geq \Omega\left(K^{\frac{3\epsilon'}{2}}\right).$$

This concludes that this term grows as $K \rightarrow \infty$. It can be verified that in general if $A = B \cdot Z$, where B is a constant and Z is a random variable with continuous PDF, then as $B \rightarrow \infty$, $\mod(A, 2\pi) \rightarrow \mathcal{U}(0, 2\pi)$. Consequently

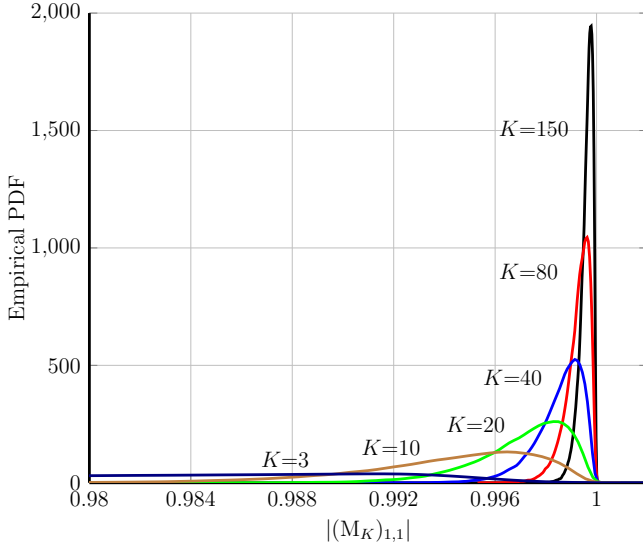
$$\mod\left(\sum_{s=t_1}^{t_2-1} (\Phi_{s,1} - \Phi_{s,2}), 2\pi\right) \rightarrow \mathcal{U}(0, 2\pi).$$

Hence, the summation of terms with a distance more than $K^{1-\delta/3+\epsilon'}$ can be considered as the summation of independent random variables. Using central limit theorem yields

$$\begin{aligned} |(\Delta_r)_{1,2}| &\leq |(\mathbf{C}_1)_{1,2}| O\left(K^{2\epsilon'} K^{\delta/6} K^{1-\delta} K^{-1}\right) \\ &= O\left(K^{-5\delta/6+2\epsilon'}\right). \end{aligned}$$

This completes the proof of Claim 1.

• *Case 1 $\leq \delta < 1.5$:* Similar to the previous case, first assume that $r \leq K^{1-\delta/3-\epsilon'}$. For $i \in [r-1]$, due to the assumption of the induction (47), $v(\delta) \geq 1 - g$. Since $1 - \delta/3 < 2 - \delta$, then it can be verified similar to the previous case that the restrictive term is the signal-noise interaction term

Fig. 2: Empirical PDF of $|(M_K)_{1,1}|$ for finite dispersion.

and (45) (Claim 2) holds. Hence,

$$\sum_{i=1}^r e^{j \sum_{s=i}^r (\Phi_{s,1} - \Phi_{s,2})} = \frac{e^{j(\Phi_{1,1} - \Phi_{2,2})} (e^{jrK^{\delta-1}Q} - 1)}{K (e^{jK^{\delta-1}Q} - 1)}. \quad (53)$$

For $\delta > 1$, the above function is an oscillating function of order $O(1)$, which concludes that $v(\delta) = 1 - g$ for r steps as well, when $r \leq K^{1-\delta/3-\epsilon'}$. This proves Claim 3 and consequently Claim 1 for $r \leq K^{1-\delta/3-\epsilon'}$.

For $r > K^{1-\delta/3-\epsilon'}$, similar to the previous case it can be verified that sum of each $K^{1-\delta/3-\epsilon'}$ consecutive terms is $O(K^g)$. Thus,

$$|(\Delta_r)_{1,2}| \leq |(C_1)_{1,2}| O\left(K^{\delta/3-1+g+\epsilon'}\right).$$

Furthermore, using the central limit theorem, this bound can be improved to

$$|(\Delta_r)_{1,2}| \leq |(C_1)_{1,2}| O\left(K^{\delta/6-1+g+2\epsilon'}\right),$$

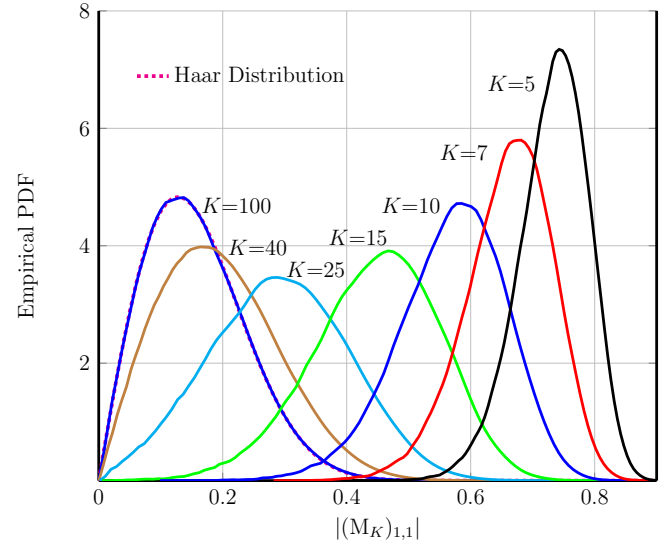
which completes proof of Claim 1.

• *Case 1.5 $\leq \delta < 2$:* Since $2 - \delta < 1 - \delta/3$, in this regime, the intra-channel term is the restrictive term. In this case, it can be verified that $r \leq K^{2-\delta-\epsilon'}$ consecutive terms form geometric series and their sum is $O(K^g)$ (Claims 2 and 3). Hence, to show Claim 1, $|(\Delta_r)_{1,2}|$ can be bounded as:

$$\begin{aligned} |(\Delta_r)_{1,2}| &\leq |(C_1)_{1,2}| O\left(K^{2\epsilon'+g} K^{\frac{1-(2-\delta)}{2}} K^{-1}\right) \\ &= |(C_1)_{1,2}| O\left(K^{\delta/2-1.5+g+2\epsilon'}\right). \end{aligned}$$

• *Cases 2 $\leq \delta < 3$ and 3 $\leq \delta$:* For these cases, first we argue that when (44) holds, then as $K \rightarrow \infty$, $\text{mod}(\Phi_{r,l}, 2\pi) \rightarrow \mathcal{U}(0, 2\pi)$, independent of $(\Phi_{i,l})_{i=1}^{r-1}$. In other words, in this regime as $K \rightarrow \infty$, SSFM channel converges to the finite dispersion fading channel, except for the first segment and when $2 < \delta < 3$, which is negligible. This, concludes that

$$\Delta_r = \frac{O(\sqrt{r})}{K} = O\left(K^{-1/2}\right),$$

Fig. 3: Empirical PDF of $|(M_K)_{1,1}|$ for infinite dispersion.

which completes the proof of Claim 1. Note that Claims 2 and 3 are valid only for $\delta < 2$.

For $2 \leq \delta < 3$, the second phase operator is equal to

$$\begin{aligned} \Phi_{2,l} &= \gamma\mu \sum_{t=1}^M \left| X_l + \frac{(C_1 \mathbf{X})_l}{K} + \mathbf{Z}_1 + O\left(\frac{1}{K^2}\right) + W_{2,l}(t) \right|^2 \\ &\approx \gamma\epsilon |X_{1,l}|^2 + \frac{\gamma\mathcal{L}}{K^2} X_{1,l} (C_1 \mathbf{X})_l. \end{aligned}$$

For i.i.d. inputs, the second term induces a stochastic impairment that grows if $\delta > 2$ and when $K \rightarrow \infty$.

Hence, as $K \rightarrow \infty$, each step will be reduced to uniform phase noise. Similarly, after r steps, there would be a stochastic impairment of order $\frac{\sqrt{r}}{K} \|X\|_4$. Thus, the channel (except for the first segment) is equivalent to the fading channel.

For $3 \leq \delta$, SSFM channel converges to the fading channel for any input distribution that escapes to infinity, as $K \rightarrow \infty$. To show this, first using the assumption of the induction, for $1 \leq i \leq r$, we have

$$|V_{r,l}| = K^{\delta/2} |X'_l| + O\left(K^{\delta/2-0.5}\right).$$

Hence, the second term of $\Phi_{r,1}$, i.e. $2\gamma\epsilon\sqrt{\epsilon}\Re(V_{r,l}Z'_{r,l})$, which conditioned on other segments and coordinates is not deterministic, grows unboundedly. Thus, $\text{mod}(\Phi_{r,l}, 2\pi) \rightarrow \mathcal{U}(0, 2\pi)$. This completes the proof.

E. Proof of Theorem 1

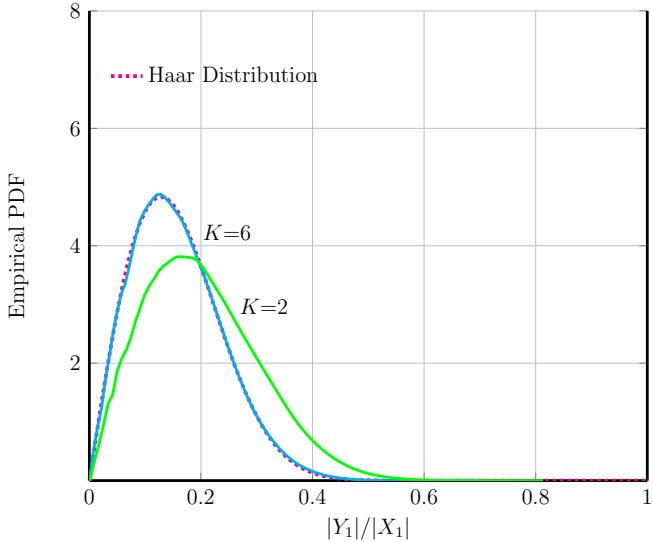
Let $\mathbf{Y}' \triangleq \mathbf{R}(\boldsymbol{\theta})\mathbf{Y}$, where $\theta_l \stackrel{\text{i.i.d.}}{\sim} \mathcal{U}(0, 2\pi)$. Due to data processing inequality

$$I(\mathbf{Y}; \mathbf{X}) \geq I(\mathbf{Y}'; \mathbf{X}).$$

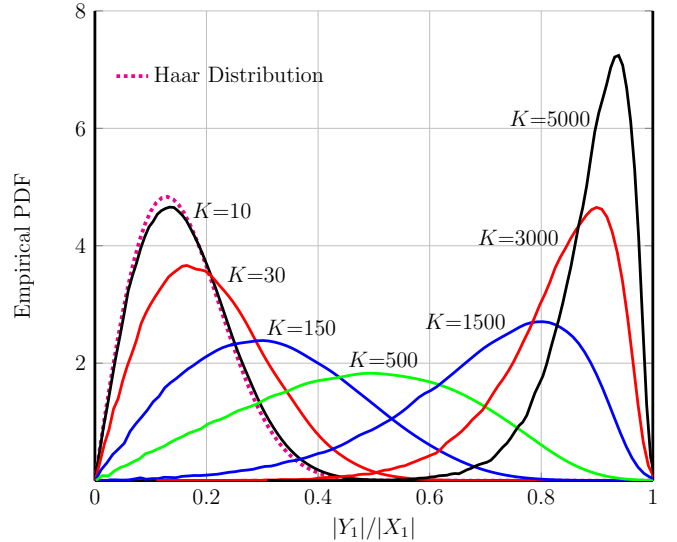
In the following, we establish a lower bound on the channel $\mathbf{X} \mapsto \mathbf{Y}'$.

The channel $\mathbf{X} \mapsto \mathbf{Y}'$ when $K \rightarrow \infty$, is

$$\mathbf{Y}' = \mathbf{M}_K \mathbf{X} + \mathbf{Z},$$



(a) First, PDF gets close to Haar distribution.



(b) Then, PDF converges to δ(w - 1).

Fig. 4: Empirical PDF of $|(\mathbf{M}_K)_{1,1}|$ for finite dispersion.

where

$$\mathbf{M}_K \stackrel{d}{=} e^{\zeta} \mathbf{R}(\boldsymbol{\theta}) + O\left(K^{-v(\delta)}\right).$$

If $v(\delta) < \frac{1}{2}\delta$, then the term $O(K^{-v(\delta)}) \mathbf{X}$ vanishes as $K \rightarrow \infty$ and the channel tends to n independent phase noise channels. The result then can be established similar to Theorem 2.

If $v(\delta) > \frac{1}{2}\delta$, an approach similar to that in the proof of Theorem 3 can be applied. The output entropy $h(\mathbf{Y}')$ can be bounded as in (38). Bounding the conditional part also follows similarly as in the proof of Theorem 3, with the difference that the defined variable T_l is not anymore Gaussian, and is a random variable with bounded variance $\sigma_{T_l}^2$. Applying the maximum entropy theorem, the conditional entropy can be similarly bounded as

$$\begin{aligned} h(Y_l'|\mathbf{X}) &\leq \log_2 \left(\frac{2e^\zeta \pi}{K^{v(\delta)}} \right) + O\left(\sqrt{\frac{K}{\mathcal{P}}}\right) + O\left(\frac{1}{\sqrt{K}}\right) \\ &\quad + \mathbb{E}[\log_2(|X_l| \|\mathbf{X}\|_4)] + \frac{1}{2} \log_2(2\pi e \sigma_{T_l}^2). \end{aligned}$$

This relation together with (38) and (39), and letting $\mathbf{X} = \mathcal{N}_{\mathbb{C}}(0, \mathcal{P}_{\mathbf{I}_n})$, complete the proof.

VII. SIMULATION EXPERIMENTS

The capacity results in Section V are supported by numerical simulation, that are presented below for the fading and SSFM models.

A. Fading Channel

In the first experiment, we simulate random matrix \mathbf{M}_K for finite dispersion case with zero loss, $n = 32$, and for values of b_l in (12) with $T \triangleq n\Delta_t = 50$, $\beta_2 = -2$, and $\mathcal{L} = 1/4$. Fig 2 shows that the empirical PDF of $W \triangleq |(\mathbf{M}_K)_{1,1}|$ converges to the Dirac delta function $\delta(W - 1)$, which is explained by

Lemma 1. For these choices of b_l , which have small absolute values, PDF of $|(\mathbf{M}_K)_{1,1}|$ gets increasingly closer to $\delta(W - 1)$ as K increases.

In the second experiment, matrix \mathbf{M}_k is simulated for infinite dispersion case with zero loss and $n = 32$. In this simulation values of b_l are chosen to be some constants in the interval $(0, \pi/3]$ such that the matrix \mathbf{D} becomes a non-block diagonal matrix. Fig 3 shows that the empirical PDF of $W \triangleq |(\mathbf{M}_K)_{1,1}|$ converges to the PDF of $\hat{W} = |\mathbf{M}_{1,1}|$, where \mathbf{M} is distributed according to the Haar measure over the group of unitary matrices. This confirms the result of Lemma 3. Note that, by Theorem 9 in Appendix A, $P_{\hat{W}}(\hat{w}) = 2(n-1)\hat{w}(1-\hat{w}^2)^{n-2}$.

In the third experiment, the first simulation is repeated with the same parameters except for $\mathcal{L} = 25$, which results in larger absolute values for b_l . In this case, as K is increased, the empirical PDF of W first, very fast as shown in Fig. 4a, gets close to the PDF of \hat{W} , which by Lemma 3 corresponds to the PDF of $|(\mathbf{M}_K)_{1,1}|$ in infinite dispersion fading channel when $K \rightarrow \infty$. Hence, it seems that when $|b_l|$ are not small, the PDF of $|(\mathbf{M}_K)_{1,1}|$ in the fading channel with finite dispersion is similar to the infinite dispersion case.

As K is further increased, the distribution of \mathbf{M}_K gets far from PDF of \hat{W} ; as a consequence, as it can be observed in Fig. 4b, the PDF of W tends to $\delta(W - 1)$ rather than (56).

B. SSFM Channel

In the first experiment, to verify the convergence of SSFM channel to a diagonal model when K is sufficiently large, a lossless channel is simulated for 1000 realizations of the noise and large input $X_l \stackrel{\text{i.i.d.}}{\sim} 10^8(\mathcal{U}(0, 1) + 0.7)$. We compute the empirical PDF of $|Y_1|/|X_1|$. The number of spatial segments K is chosen as follows. Considering the proof of Lemma 1 in Section VI, the SSFM model is diagonal when C_1/\sqrt{K} is small, where the matrix C_1 is defined in (36). Hence, $\frac{1}{\sqrt{K}} \max_l |d_l|$ should be small, e.g., less than 0.1. For the

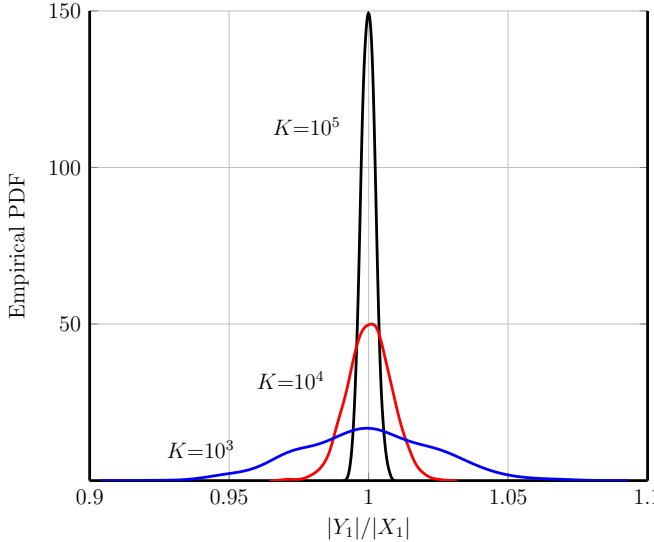


Fig. 5: Empirical PDF of $|Y_1|/|X_1|$ for SSFM channel with $n = 32$.

normalized NLS equation in [17], $\max_l |d_l| = (n\pi/T)^2$. Letting $T = 50$, we obtain $K \geq 16(n/10)^4$.

Example n=32: In this case, $K > 1500$. Fig. 5, shows that the empirical PDF of $|Y_1|/|X_1|$ is concentrated around 1, with $\sigma^2 = 5 \times 10^{-5}$. This supports the relation $|Y_1| \approx |X_1|$ with probability one as $K \rightarrow \infty$.

Example n=1024: In this case, $K > 1.7 \times 10^9$ and simulation is infeasible. However, if we reduce d_l by factor 100 (or 400), we obtain $K > 10^4$ (or $K > 1.7 \times 10^5$). Fig. 6b shows the empirical PDF of $|Y_1|/|X_1|$ for several values of K and $\sigma^2 = 1.5 \times 10^{-3}$, demonstrating $|Y_1| \approx |X_1|$.

In the second experiment, we investigate the rate of convergence of the SSFM channel to the diagonal phone noise model. We consider normalized SSFM with $n = 32$, $K = 10^4$, $\sigma^2 = 5 \times 10^{-5}$, and 1000 realizations of the noise and input $X_l \stackrel{\text{i.i.d.}}{\sim} \sqrt{\frac{P}{1.5}}(\mathcal{U}(0, 1) + 0.7)$, where $P = K^\delta$, for $0 \leq \delta \leq 4$. Define

$$v(\delta) \triangleq -\log_K \left(\frac{1}{K} \sum_{i=1}^r e^{j \sum_{l=i}^K (\Phi_{l,1})} \right).$$

This quantity, as explained in (50), shows the rate of convergence of M_K to $e^{\zeta+jd}S_K$. In Fig. 7, $v(\delta)$ is simulated. The results are compatible with Lemma 4. Moreover, it can be seen in the proof of Lemma 4 that for small values of $\sigma^2 \mathcal{L}$, the signal-noise interaction may not be dominant except for very large K , when $K \gg (\gamma \mathcal{L}^{3/2} \sigma)^{-2/\delta}$.

When $\gamma \mathcal{L}^{3/2} \sigma K^{\delta/2}$ is small, $v(\delta)$ can be lower bounded as

$$v(\delta) + \varepsilon' \geq \begin{cases} \delta, & 0 \leq \delta \leq 1, \\ 1.5 - \delta/2 - g, & 1 \leq \delta \leq 2 \\ & \text{and i.i.d. input,} \\ 0.5, & 2 \leq \delta \leq 3 \\ & \text{and i.i.d. input,} \\ 0.5, & 3 \leq \delta, \end{cases} \quad (54)$$

which is compatible with the simulation result in Fig. 7. The oscillation for $1 \leq \delta \leq 2$ is also explained by Lemma 4 and in particular (53).

In the last experiment, the effect of loss is examined. The previous experiment is repeated with fixed $\delta = 0.6$ and $\zeta = -1.35$. For $K = 100$, $K = 1000$, and $K = 10000$, the convergence rate $v(\delta)$ are 0.463, 0.512, and 0.534, respectively. This is explained by (51), implying that for $0 < \delta < 1$ and small noise power, $v(\delta) = \delta + 2a\zeta/\ln K \rightarrow \delta$, where a is a value less than 1. In our experiment, $a \approx 0.23$.

VIII. CONCLUSION

The capacity $\mathcal{C}(\mathcal{P})$ of the discrete-time continuous-space SSFM model of the optical fiber is considered as a function of the average power \mathcal{P} . We considered the asymptotic capacity when $\mathcal{P} \rightarrow \infty$, and the number of spatial segments in SSFM is $K \geq \sqrt[3]{\mathcal{P}}$, $\delta > 0$.

First, we showed that if $\delta < 3/2$, namely, when K is sufficiently large, then $\mathcal{C}(\mathcal{P}) \geq \frac{1}{2} \log_2(1 + \text{SNR}) + O(1)$. As a result, the number of signal DoFs is at least half of the input dimension. If $\delta \in [3/2, 2]$ or $\delta > 2$, the pre-logs in the capacity lower bound are respectively $(3 - \delta)/2\delta$ or $1/2\delta$.

Second, we considered a variant of the SSFM model where the dispersion matrix in each segment does not depend on K . It is shown that when $K \geq \mathcal{P}^{1/3}$ and $\mathcal{P} \rightarrow \infty$, $\mathcal{C}(\mathcal{P}) = \frac{1}{2n} \log_2(1 + \text{SNR}) + o(1)$. In this model, there is exactly one signal DoF.

Finally, it is shown that the capacity of continuous-space SSFM channel when $\gamma = \infty$ is $\frac{1}{2} \log_2(1 + a \text{SNR}) + o(1)$. Hence, the number of signal DoFs is exactly half of the input dimension.

APPENDIX A

MATHEMATICAL PRELIMINARIES

A. Spherical Coordinate System

The n -dimensional spherical coordinate system is described by a radius, r , and $n-1$ angles θ_i , $i \in [n-1]$, where $\theta_i \in [0, \pi]$ for $i \in [n-2]$, and $\theta_{n-1} \in [0, 2\pi]$. A vector $\mathbf{x} \in \mathbb{R}^n$ can be written in the spherical coordinate as

$$\begin{aligned} x_1 &= r \cos(\theta_1), \\ x_i &= r \cos(\theta_i) \prod_{r=1}^{i-1} \sin(\theta_r), \quad i = 2, \dots, n-2 \\ x_{n-1} &= r \prod_{r=1}^{n-1} \sin(\theta_r). \end{aligned}$$

Alternatively, we denote \mathbf{x} by its norm $\|\mathbf{x}\|$ and direction $\hat{\mathbf{x}} = \mathbf{x}/\|\mathbf{x}\|$ on the surface of the $n-1$ -sphere

$$\mathcal{S}^{n-1} = \{\mathbf{x} \in \mathbb{R}^n : \|\mathbf{x}\| = 1\}.$$

Complex vectors in \mathbb{C}^n can be similarly represented.

B. Groups

The reader is referred to [18]–[20] for background on group theory. For a group G , notation $H \leq G$ is used to say that H

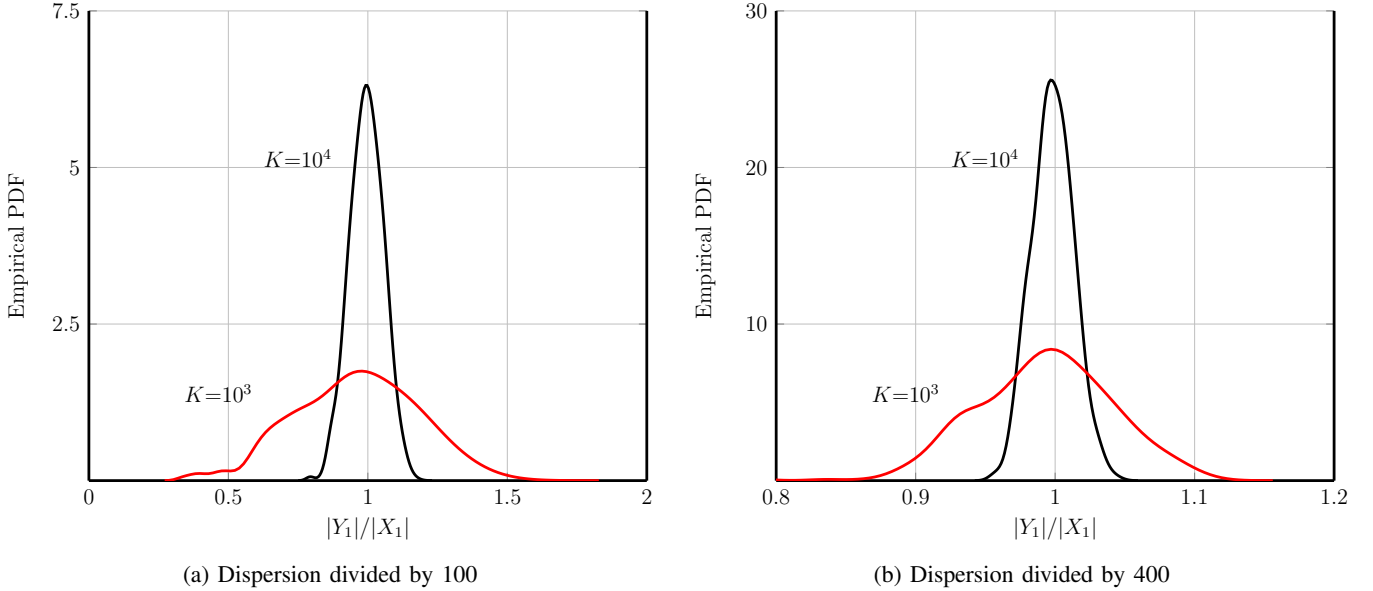


Fig. 6: Empirical PDF of $|Y_1|/|X_1|$ for SSFM channel with $n = 1024$ and dispersion coefficients divided by 100 and 400.

is a subgroup of G and gH and Hg are respectively the left coset and right coset of H w.r.t. $g \in G$.

A probability measure on G is a non-negative, real-valued, countably additive, regular Borel measure μ on G , such that $\mu(G) = 1$. The support of μ , denoted by $\mathcal{S}(\mu)$ is the smallest closed subset of G of μ -measure.

A probability measure μ on G is said to be (normally) aperiodic if its support is not contained in a (left or right) coset of a proper closed (normal) subgroup of G .

a) *Group of Unitary Matrices:* The group that we are interested in this paper is the group of unitary matrices. A matrix $U \in \mathbb{C}^{n \times n}$ is unitary if

$$UU^H = U^H U = I_n,$$

where U^H denotes the conjugate transpose of U . The set of unitary matrices in $\mathbb{C}^{n \times n}$ with matrix multiplication forms a group \mathbb{U}_n , which is a compact Lie group.

The following theorem is a re-statement of [21, Thm. 1], bringing parts of its proof to the theorem statement.

Theorem 7. Suppose that a subgroup $\mathbb{H} \leq \mathbb{U}_n$ contains the subgroup of diagonal matrices. Let ν be a binary relation on $\mathcal{I}_n = \{1, 2, \dots, n\}$ defined as follows: $\forall r, s \in [n]$, $r \stackrel{\nu}{\sim} s$ if and only if there exists a matrix $A \in \mathbb{H}$ and $t \in [n]$ such that $A_{r,t} \neq 0$ and $A_{s,t} \neq 0$.

Then, we have

- i. ν is an equivalence relation on \mathcal{I}_n ,
- ii. $\mathbb{U}_n(\nu) \leq \mathbb{H}$.

C. Haar Measure

This subsection is borrowed mainly from [22]. Haar measure can be seen as an extension of the notion of the uniform random variable over an interval. The extension is based on the shift invariant property of the uniform random variable. If $X \sim \mathcal{U}(0, a)$, then for any $b \in \mathbb{R}$, $\text{mod}(X + b, a) \sim \mathcal{U}(0, a)$.

Consider defining uniform distribution on the circle \mathcal{S}^1 in \mathbb{R}^2 . Considering a circle as a geometric object, a “uniform random point on the circle” should be a complex random variable whose distribution is rotation invariant; that is, if $A \subseteq \mathcal{S}^1$, then the probability of the random point lying on A should be the same as the probability that it lies on $e^{j\theta}A = \{e^{j\theta}a : a \in A\}$.

The uniform distribution μ on a group G is called Haar measure on G , defined based on the “translation-invariant” property as follows. For a group (G, \cdot) , an element $g \in G$, and a Borel subset $\mathcal{S} \subseteq G$, the left translation of \mathcal{S} by g is defined as

$$g\mathcal{S} = \{g \cdot s : s \in \mathcal{S}\}.$$

A measure μ on the Borel subsets of G is called left translation-invariant if for all Borel subsets $\mathcal{S} \subseteq G$ and all $g \in G$,

$$\mu(g\mathcal{S}) = \mu(\mathcal{S}).$$

Right translation and right translation-invariant are defined similarly.

There exists a unique Haar measure on any group. The following theorem is proved in [22, Lemma 2.1.] for $G = \mathbb{U}_n$.

Theorem 8. There exists a unique (left or right) translation-invariant probability measure on \mathbb{U}_n , called Haar measure.

Let $M \in \mathbb{C}^{n \times n}$ be a random unitary matrix, $W_l \triangleq |M_{l,1}|$, and $\mathbf{W} = (W_1, \dots, W_n)$.

Theorem 9. Suppose that M is distributed according to Haar measure on the group of random unitary matrices. Then,

$$P_{\mathbf{W}}(\mathbf{w}) = 2^{n-1}(n-1)! \prod_{l=1}^{n-1} w_l. \quad (55)$$

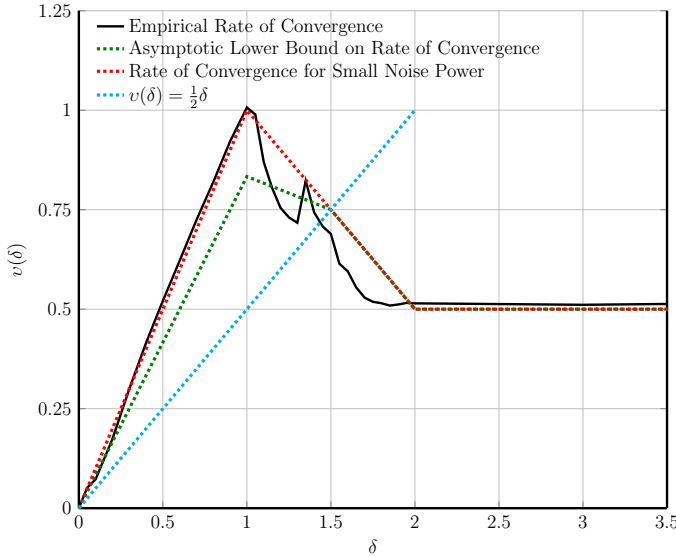


Fig. 7: Rate of Convergence of SSFM channel to the diagonal model for $n = 32$, $K = 10^4$, and $\mathcal{P} = K^\delta$.

Proof. Let $W_l = R_l + jT_l$, $R_l, T_l \in \mathbb{R}$, $l \in [n]$. The vector

$$(R_1, \dots, R_n, T_1, \dots, T_n)$$

has the uniform distribution over S_{2n-1} . From [23, Eq.1.26.], the joint distribution of (R_1, T_1) is

$$P_{R_1, T_1}(r_1, t_1) = \frac{\Gamma(n)}{\Gamma(n-1)\pi} (1 - (r_1^2 + t_1^2))^{n-2}.$$

Since the phase is uniform, we get

$$P_{W_1}(w_1) = 2(n-1)w_1 (1 - w_1^2)^{n-2}.$$

Similarly, the joint distribution of (R_1^2, T_1^2) is

$$P_{R_1^2, T_1^2}(r_1^2, t_1^2) = \frac{\Gamma(n)}{\Gamma(n-2)\pi^2} (1 - (r_1^2 + t_1^2 + r_2^2 + t_2^2))^{n-3}.$$

Again since phase is uniform, then

$$P_{W_1^2}(w_1^2) = 2^2(n-1)(n-2)w_1 w_2 (1 - (w_1^2 + w_2^2))^{n-3}.$$

The result can be similarly established for W_1^n by induction. \square

The joint PDF (55) gives the marginal $P_{W_1}(w_1) = g(w_1, n)$, where

$$g(w, n) \triangleq 2(n-1)w(1 - w^2)^{n-2}.$$

The conditional PDFs for $l = 2, \dots, n$ are

$$\begin{aligned} P_{W_l | W_1^{l-1}}(w_l | w_1^{l-1}) &= \left(1 - \sum_{l=1}^{l-1} w_l^2\right)^{-\frac{1}{2}} \\ &\times g\left(\left(1 - \sum_{l=1}^{l-1} w_l^2\right)^{-\frac{1}{2}} w_l, n - l + 1\right). \end{aligned} \quad (56)$$

Theorem 10. Suppose that $\mathbf{M} \in \mathbb{C}^{n \times n}$ is distributed according to the Haar measure on \mathbb{U}_n . Then, $P_{\mathbf{M}\mathbf{x}|\mathbf{x}}(\mathbf{M}\mathbf{x}|\mathbf{x})$ is independent of \mathbf{x} .

Proof. Fix an orthonormal basis V_1, \dots, V_n of \mathbb{C}^n such that $V_1 = \mathbf{x}$. Denote the matrix with columns V_i by Λ . Assume that \mathbf{M} is a unitary matrix distributed according to Haar measure. Define the map $\Phi : \mathbb{C}^{n \times n} \mapsto \mathbb{C}^{n \times n}$ as

$$\mathbf{M}' = \mathbf{M}\Lambda.$$

Thus,

$$P(\mathbf{M}\mathbf{x}|\mathbf{x}) = P(\mathbf{M}'\mathbf{x}'|\mathbf{x}' = (1, 0, \dots, 0)^T),$$

Since Φ is invertible, then \mathbf{M}' is also distributed according to Haar measure and the RHS of above is derived in Theorem 9. This proves that $P(\mathbf{M}\mathbf{x}|\mathbf{x})$ does not depend on \mathbf{x} . \square

D. Random Walk on Groups

This section is mainly from [19]. A random walk on a group (G, \cdot) is

$$S_K = X_K \cdot X_{K-1} \cdots X_1, \quad K = 1, 2, \dots, \quad (57)$$

where $X_i \stackrel{\text{i.i.d.}}{\sim} \mu(G)$. If X and y are random variables on G with PDF μ and ν respectively, then PDF of $X \cdot Y$ is $\mu * \nu$, where $*$ denotes the convolution. Hence, the PDF of S_K is the K -th convolution power of μ , denoted by μ^{*K} .

The following theorem is proved by Kawada and Itô for compact metric groups [24]. A more general version is proved by Stromberg in [20, Thm. 3.3.5] for Hausdorff groups, where the aperiodic condition is replaced with the normally aperiodic condition.

Theorem 11 (Kawada-Itô and Stromberg). *Let G be a compact Hausdorff groups and H the smallest closed subgroup of G which contains $\mathcal{S}(\mu)$. Then, $\lim_{K \rightarrow \infty} \mu^{*K}$ exists if and only if μ is a normally aperiodic probability measure on subgroup H . Moreover, if this limit exists, then it is the Haar measure on H .*

Proof. See [20, Thm. 3.3.5]. \square

ACKNOWLEDGEMENT

This work has received funding from the European Research Council (ERC) under the European Union's Horizon 2020 research and innovation programme, Grant Agreement No. 805195. The authors are greatly thankful to Emmanuel Breuillard for sharing his helpful ideas.

REFERENCES

- [1] C. E. Shannon, "The mathematical theory of communication," *Bell Syst. Tech. J.*, vol. 27, pp. 379–423, Jul. 1948.
- [2] M. I. Yousefi and F. R. Kschischang, "On the per-sample capacity of nondispersive optical fibers," *IEEE Trans. Inf. Theory*, vol. 57, no. 11, pp. 7522–7541, Nov. 2011.
- [3] A. Splett, C. Kurzke, and K. Petermann, "Ultimate transmission capacity of amplified optical fiber communication systems taking into account fiber nonlinearities," in *European Conf. Opt. Commun.*, Sep. 1993, pp. 1–3.
- [4] P. P. Mitra and J. B. Stark, "Nonlinear limits to the information capacity of optical fiber communications," *Lett. Nature*, vol. 411, pp. 1027–1030, Jun. 2001.
- [5] R. J. Essiambre, G. Kramer, P. J. Winzer, G. J. Foschini, and B. Goebel, "Capacity limits of optical fiber networks," *IEEE J. Lightw. Technol.*, vol. 28, no. 4, pp. 662–701, Feb. 2010.

- [6] M. Secondini, E. Forestieri, and G. Prati, "Achievable information rate in nonlinear wdm fiber-optic systems with arbitrary modulation formats and dispersion maps," *IEEE J. Lightw. Technol.*, vol. 31, no. 23, pp. 3839–3852, Dec. 2013.
- [7] M. I. Yousefi, G. Kramer, and F. R. Kschischang, "Upper bound on the capacity of the nonlinear Schrödinger channel," in *Canadian Workshop on Inf. Theory*, St. John's, Newfoundland, Canada, Jul. 2015, pp. 1–5.
- [8] G. Kramer, M. I. Yousefi, and F. Kschischang, "Upper bound on the capacity of a cascade of nonlinear and noisy channels," in *IEEE Inf. Theory Workshop*, Jerusalem, Israel, Apr. 2015, pp. 1–4.
- [9] K. S. Turitsyn, S. A. Derevyanko, I. V. Yurkevich, and S. K. Turitsyn, "Information capacity of optical fiber channels with zero average dispersion," *Phys. Rev. Lett.*, vol. 91, no. 20, p. 203901, Nov. 2003.
- [10] A. V. Reznichenko and I. S. Terekhov, "Path integral approach to nondispersive optical fiber communication channel," *Entropy*, vol. 22, no. 6, May 2020.
- [11] K. Keykhosravi, G. Durisi, and E. Agrell, "Accuracy assessment of nondispersive optical perturbative models through capacity analysis," *Entropy*, vol. 21, no. 8, Aug. 2019.
- [12] M. I. Yousefi, "The asymptotic capacity of the optical fiber," arXiv:1610.06458, Nov. 2016.
- [13] K. Keykhosravi, E. Agrell, and G. Durisi, "Rates achievable on a fiber-optical Split-Step Fourier channel," arXiv:1512.01843, Oct. 2016.
- [14] S. M. Moser, "Duality-based bounds on channel capacity," Ph.D. dissertation, ETH Zurich, Switzerland, Jan. 2005.
- [15] A. Lapidot, "On phase noise channels at high SNR," in *IEEE Inf. Theory Workshop*, Oct. 2002, pp. 1–4.
- [16] H. Ghouchian, A. Gohari, and A. Amini, "Existence and continuity of differential entropy for a class of distributions," *IEEE Commun. Lett.*, vol. 21, no. 7, pp. 1469–1472, 2017.
- [17] M. I. Yousefi and F. R. Kschischang, "Information transmission using the nonlinear Fourier transform, Part I, II, III," *IEEE Trans. Inf. Theory*, vol. 60, no. 7, pp. 4312–4369, Jul. 2014.
- [18] J. F. Quint, "An introduction to random walks on groups," *School on Inf. and Randomness*, Dec. 2014.
- [19] E. Breuillard, "Random walks on Lie groups," *Lecture Notes*, Mar. 2004.
- [20] K. Stromberg, "Probabilities on a compact group," *Trans. Am. Math. Soc.*, vol. 94, no. 2, pp. 295–309, 1960.
- [21] Z. Borevich and S. Krupetskii, "Subgroups of the unitary group that contain the group of diagonal matrices," *J. Sov. Math.*, vol. 17, no. 4, pp. 1951–1959, 1981.
- [22] E. S. Meckes, *The Random Matrix Theory of the Classical Compact Groups*. Cambridge Univ. Press, 2019.
- [23] K. T. Fang, S. Kotz, and K. Wangng, *Symmetric multivariate and related distributions*. Taylor & Francis, Jan. 2018.
- [24] Y. Kawada and K. Itô, "On the probability distribution on a compact group," *I. Proc. Phys.-Math. Soc. Japan*, vol. 22, no. 3, pp. 977–998, 1940.